

Review

Research Progress on Thermal Conductivity of High-Pressure Die-Cast Aluminum Alloys

Yixian Liu ¹ and Shoumei Xiong ^{1,2,*}

¹ School of Materials Science and Engineering, Tsinghua University, Beijing 100084, China; liu-yx20@mails.tsinghua.edu.cn

² Key Laboratory for Advanced Materials Processing Technology, Tsinghua University, Beijing 100084, China

* Correspondence: smxiong@tsinghua.edu.cn; Tel.: +86-10-62773793

Abstract: High-pressure die casting (HPDC) has been extensively used to manufacture aluminum alloy heat dissipation components in the fields of vehicles, electronics, and communication. With the increasing demand for HPDC heat dissipation components, the thermal conductivity of die-cast aluminum alloys is paid more attention. In this paper, a comprehensive review of the research progress on the thermal conductivity of HPDC aluminum alloys is provided. First of all, we introduce the general heat transport mechanism in aluminum alloys, including electrical transport and phonon transport. Secondly, we summarize several common die-cast aluminum alloy systems utilized for heat dissipation components, such as an Al-Si alloy system and silicon-free aluminum alloy systems, along with the corresponding composition optimizations for these alloy systems. Thirdly, the effect of processing parameters, which are significant for the HPDC process, on the thermal conductivity of HPDC aluminum alloys is discussed. Moreover, some heat treatment strategies for enhancing the thermal conductivity of die-cast aluminum alloys are briefly discussed. Apart from experimental findings, a range of theoretical models used to calculate the thermal conductivity of die-cast aluminum alloys are also summarized. This review aims to guide the development of new high-thermal-conductivity die-cast aluminum alloys.

Keywords: high-pressure die casting; aluminum alloy; thermal conductivity; alloy development



Citation: Liu, Y.; Xiong, S. Research Progress on Thermal Conductivity of High-Pressure Die-Cast Aluminum Alloys. *Metals* **2024**, *14*, 370. <https://doi.org/10.3390/met14040370>

Academic Editor: Menachem Bamberger

Received: 19 February 2024

Revised: 11 March 2024

Accepted: 17 March 2024

Published: 22 March 2024



Copyright: © 2024 by the authors. Licensee MDPI, Basel, Switzerland. This article is an open access article distributed under the terms and conditions of the Creative Commons Attribution (CC BY) license (<https://creativecommons.org/licenses/by/4.0/>).

1. Introduction

Presently, aluminum and aluminum alloys are significant metallic materials because of their outstanding advantages such as high specific strength, great corrosion resistance, low density, exceptional thermal conductivity, ease of processing, and abundant resources in the Earth's crust [1–6]. Recently, to address the increasingly severe environmental and energy challenges, the lightweight concept was proposed and applied rapidly in the automobile industry. The density of the aluminum is only $\sim 2.7 \text{ g cm}^{-3}$ [3], which causes aluminum alloys to gradually replace steel on the structural parts of automobiles to reduce CO₂ emissions and energy consumption [7]. Moreover, aluminum is also known as a green metal because it is recyclable to cyclic utilization all the time [8]. The trend of the lightweight and environmentally friendly requirement further broadens the manufacture and applications of aluminum alloys in modern industries. Particularly, compared with other metals [9–11], as shown in Figure 1, aluminum has an excellent thermal conductivity of $237 \text{ W m}^{-1} \text{ K}^{-1}$ with a low density. Aluminum alloys are extensively used in the thermal management field to produce heat dissipation components. Correspondingly, thermal conductivity of aluminum alloys is an important consideration to meet different heat conduction requirements. Therefore, thermal conductivity of aluminum alloys has become a research frontier and a focused area in the structural aluminum alloy field.

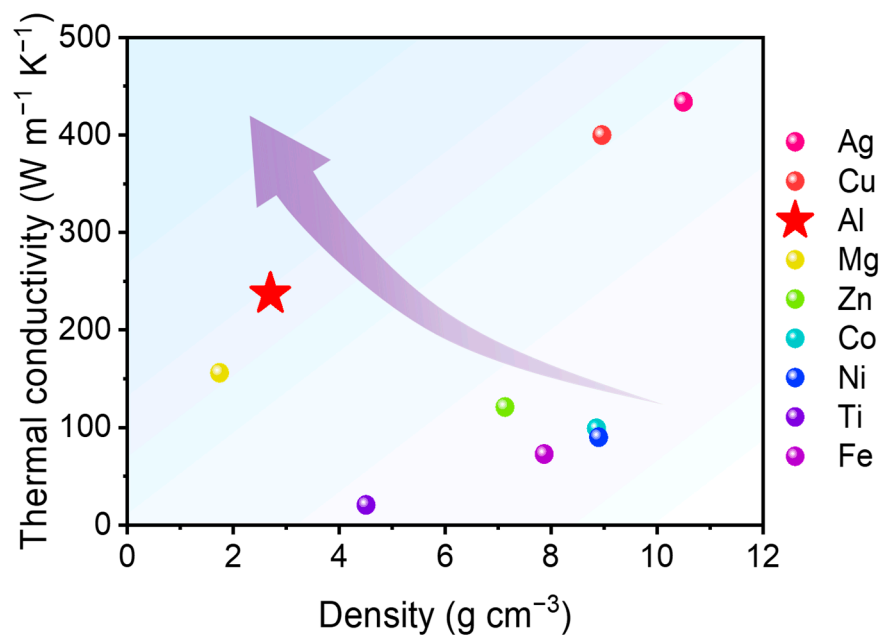


Figure 1. Density and thermal conductivity of several pure metals, adapted from [9–11].

Among all casting techniques for aluminum alloys, high-pressure die casting stands out as a near-net-shape forming technology extensively used for light metals such as Al, Mg, and Zn alloys [12]. It is one of the most common and efficient methods for mass-produced aluminum products. HPDC is capable of producing aluminum castings with complex and thin-wall structures, high dimensional accuracy, and low surface roughness [13–15]. The whole process of HPDC is shown in Figure 2 [16]. The melt during HPDC process mainly undergoes three periods: slow-shot filling in the shot sleeve, fast-shot filling in the die cavity, and a pressure intensification period in the die cavity. Initially, the mold is closed and the aluminum melt is poured into the shot sleeve (see Figure 2a). Then, the melt in the injection chamber is pushed by a piston gradually at a slow speed until the front melt reaches the gate position of the mold (see Figure 2b,c). During this slow-shot filling period, the temperature of the melt in contact with the shot sleeve decreases below the liquidus temperature, and some of the liquid solidifies, forming primary phases, namely externally solidified crystals (ESCs). Depending on different alloy compositions, the categories of ESCs are different such as the primary α -Al phase, the primary silicon phase, and the primary iron-rich phase [17–19]. Since ESCs nucleate in the shot sleeve, they commonly exhibit large sizes in castings [20]. In the fast-shot period, the piston speed increases significantly and the liquid mixture is rapidly filled into the die cavity (see Figure 2d). Because of the high interfacial heat transfer coefficient between the die and the melt [21], the liquid mixture solidifies under a very high cooling rate [22]. At the same time, the piston transports the pressure to the solidifying casting to ensure the integrity of the castings (see Figure 2e). Hence, die castings usually have great mechanical properties. Recently, vacuum-assisted high-pressure die casting has been developed and enhances the properties of aluminum alloys further [23]. Owing to these benefits, HPDC technology has been used for industrial aluminum structural parts including heat dissipation components in automobile, communication, and consumer electronics fields (see Figure 3) such as battery pack housing in automobiles, particularly new-energy vehicles, fifth-generation (5G) base station housing in communications, and mobile phone heat exchanger components in consumer electronics products [24–26].

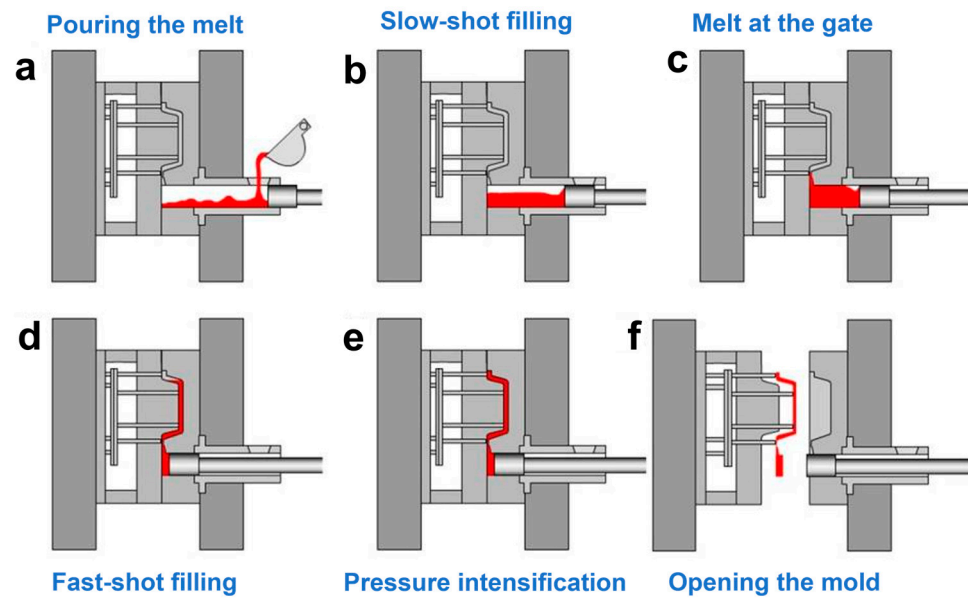


Figure 2. The process of HPDC: (a) pouring the melt; (b) slow-shot filling; (c) melt at the gate; (d) fast-shot filling; (e) pressure intensification; (f) opening the mold (reprinted with permission from ref. [16], Xiaobo Li, Tsinghua University, 2017).

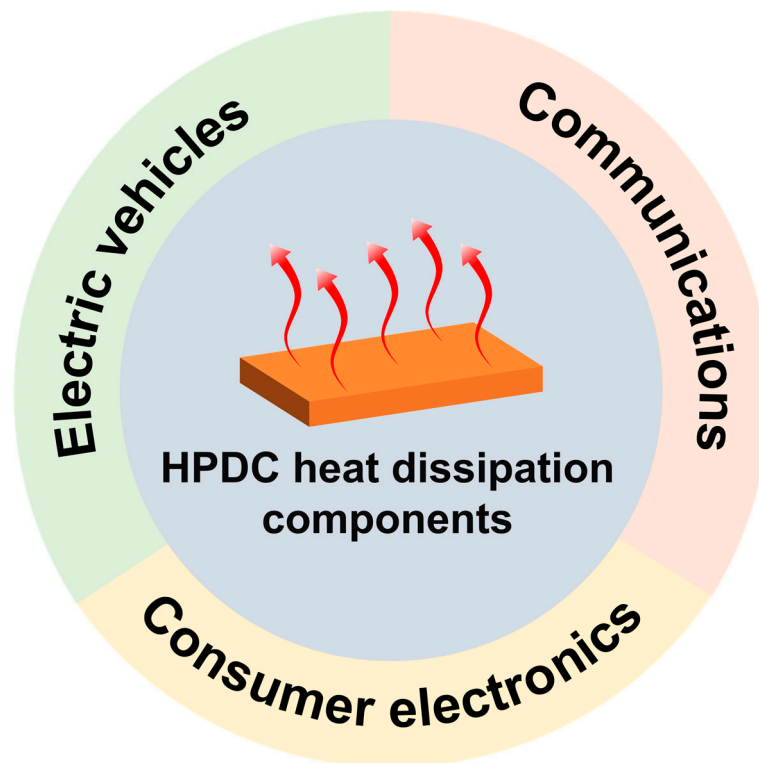


Figure 3. Applications of HPDC heat dissipation components.

In recent years, with the help of Giga Press equipment, Tesla Inc. started to implement Giga-Casting technology for the single super-sized rear floor of electric vehicles. Compared to the traditional procedure, the advanced technique can reduce costs by ~40% and weight by ~30% via producing only a single casting to replace several steel parts for a complete aluminum rear floor [27–29]. The revolutionary technology has guided many factories all over the world in the development of new electric vehicles [30–32], which brings a new development of HPDC. However, such a super-sized vehicle component does not suit the heat

treatment process used traditionally. Hence, in the HPDC field, a new frontier is the development of non-heat-treatable HPDC alloy materials, which means that alloys should have excellent properties in the as-cast state to meet the usage requirement. Worth mentioning is that non-heat-treatable HPDC alloys are proposed firstly for the Giga-Casting of electric vehicles. However, because of their advantages in cost and property, this kind of material is also imperatively needed in other structural parts like heat dissipation components.

Thermal conductivity is the most important property of a HPDC alloy in the heat dissipation component field. Table 1 shows the thermal conductivity and mechanical properties of some commercial die-cast aluminum alloys. We can see that thermal conductivity of die-cast aluminum alloys is quite low. This is because of the rapid cooling rate and the unique solidification microstructure of HPDC. The cooling rate of the HPDC process particularly in the die cavity, as shown in Figure 4, can reach up to $\sim 100 \text{ K s}^{-1}$ [22]. Hence, the solute concentrations of elements in α -Al solid solutions of die castings are usually higher than those of gravity castings [33]. Additionally, die castings have smaller grain sizes because of rapid solidification and more porosity because of melt turbulence and solidification order. Moreover, Table 1 also shows that the alloys with high thermal conductivity have low yield strength. This indicates that two crucial properties are contradictory in die-cast alloys because the requirement of precipitates and micro-defects in the alloys are truly different in thermal conductivity and strength [34].

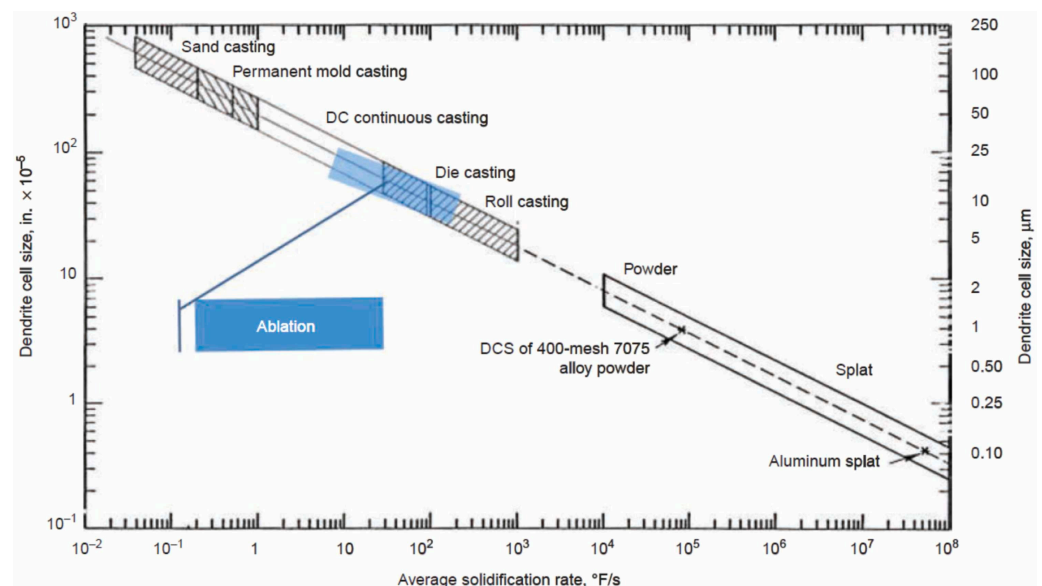


Figure 4. The solidification rate of die casting (reprinted with permission from ref. [22], 2022, Elsevier).

Table 1. Thermal conductivity and yield strength of commercial die-cast aluminum alloys.

Alloy Designation	Temper	Thermal Conductivity ($\text{W m}^{-1} \text{K}^{-1}$)	Yield Strength (MPa)	Refs.
A390	F	97	240	[35,36]
ADC12	F	92	165	[37]
A380	F	96	160	[38]
A360	F	113	170	[39]
384	F	96	170	[40]
413	F	113	145	[41]
Castasil [®] -37	F	130	135	[25]

More significantly, with the development of electronics, the power density of devices has increased, which brings about an increase in heat flow density. For electric vehicles, battery capacity increases with the emergence of plug-in hybrid electric vehicles and larger electric cars [42]. The maximum charging current and power also increase. However, the

optimal temperature range of Li-ion batteries in electric vehicles is only 15 °C~35 °C [43]. For 5G communication, the typical 5G base station will consume ~11.5 kW, which is ~70% higher than the typical 4G base station because of the extensive utilization of the Active Antenna Unit (AAU) [44]. Correspondingly, the operation frequency of 5G mobile phones is 28 or 39 GHz, which is higher than the operation frequency of ~2000 MHz for 4G phones [45], bringing more heat to be dissipated. However, the work temperature of the chips should be below 85 °C to avoid a decrease in chip performance [46]. From the facts above, there is a huge contradiction between the rapid increase in heat generation of components and the operating temperature. Therefore, the development of non-heat-treatable HPDC aluminum alloys with high thermal conductivity for heat dissipation components is truly imminent. Moreover, when improving the thermal conductivity of HPDC aluminum alloys, it is also necessary to ensure adequate mechanical properties to obtain high-performance die-cast aluminum components.

Factors affecting the thermal conductivity of HPDC aluminum alloys are numerous. The first factor is alloy composition. Generally, alloying elements in the HPDC aluminum alloy can form solid solutions via solute atoms and form precipitates via compounds. Thermal conductivity is affected by the content of these two existing states. In the die-cast industry, many studies focused on composition optimization to develop new die-cast aluminum alloys with high thermal conductivity. In addition, the properties of die-cast alloys are also influenced by die-casting process parameters. Recently, some efforts have been made to investigate the relationship between processing parameters and thermal conductivity of die-cast aluminum alloys. Furthermore, although non-heat-treatable die-cast alloys have been a trend in the HPDC industry, there is no denying that heat treatment is an effective way to improve the thermal conductivity of aluminum alloys by optimizing the microstructure [47,48]. Therefore, research on the effect of heat treatment on the thermal conductivity of die-cast aluminum alloys still holds significant value in guiding the design of new alloys. At last, as a helpful tool, theoretical models of thermal conductivity for aluminum alloys have also been employed to explain some experimental results about the relationship between the microstructure and thermal conductivity of die castings and even predict the property. Although many valuable works concerning the aspects discussed above are carried out, a systematic review about these studies on thermal conductivity of HPDC aluminum alloys is absent.

This review offers a comprehensive review of the research progress on the thermal conductivity of high-pressure die-cast aluminum alloys. Our review begins with a brief introduction of heat transport in aluminum alloys. Secondly, several common die-cast aluminum alloy systems applied for heat dissipation components are discussed. Regarding the manufacturing process, the effects of the die-casting process and heat treatment process on the thermal conductivity of HPDC aluminum alloys are summarized. Finally, the progress in theoretical models of thermal conductivity for die-cast aluminum alloys is discussed. This review provides an overview of the current research status in the field of thermal conductivity of die-cast aluminum alloys and guides the development of new high-thermal-conductivity die-cast aluminum alloys.

2. Heat Transport in Aluminum Alloys

In nature, heat transfer includes heat conduction, heat convection, and heat radiation [49]. In solids like metals, the dominant way for heat transfer is usually heat conduction. Thermal conductivity is a crucial parameter for describing and quantifying heat conduction in materials and is defined as the following equation [50]:

$$\lambda = -\frac{\vec{Q}}{\vec{\nabla}T} \quad (1)$$

where \vec{Q} is the heat flux across a unit cross section perpendicular to \vec{Q} , $\vec{\nabla}T$ is the temperature gradient, and λ is the thermal conductivity.

However, in actual heat conduction situations, it is difficult to measure the heat flux and the temperature gradient directly to obtain the thermal conductivity. Subsequently, the thermal conductivity can be written as the following equation [49]:

$$\lambda = \alpha C_p \rho \quad (2)$$

where α is the thermal diffusivity of the material, C_p is the specific heat capacity of the material, and ρ is the density of the material.

The formula can also be used to measure the thermal conductivity of metals in experiments [51]. If we consider the particles in a solid as a gas, then, according to the kinetic formula of the gas, thermal conductivity from each kind of particle can be given by the following [52]:

$$\lambda = \frac{1}{3} C v l \quad (3)$$

where C is the total heat capacity of the particles, v is the velocity of the particles, and l is the mean free distance of particles. Thermal conductivity has a positive correlation with the heat capacity, velocity, and mean free distance of particles.

For metals, the chemical bond is the metallic bond, which comprises the electrostatic attraction between free electrons and metal ions in lattice sites. Hence, heat conduction in aluminum alloys is mainly divided into two types, electron transport (the movement of free electrons) and phonon transport (the vibration of the metallic ions). Then, thermal conductivity is divided into electrical thermal conductivity and phonon thermal conductivity. A formula can express the relationship as follows [50]:

$$\lambda = \lambda_e + \lambda_p \quad (4)$$

where λ_e is the electrical thermal conductivity, and λ_p is the phonon thermal conductivity.

For the electrical thermal conductivity, a classical theory, namely the Wiedemann–Franz law, considers that the electrical thermal conductivity of aluminum alloys is linear with the electrical conductivity σ , which is easier to measure in experiments. The relationship is given by the following:

$$\lambda_e = L_0 T \sigma \quad (5)$$

where T is the absolute temperature mentioned in the Formula (1) above, and L_0 is the Lorentz constant.

The theoretical Lorentz constant is calculated by the following [53]:

$$L_0 = \frac{\pi^2 k_B^2}{3 e^2} \quad (6)$$

where e is the charge of the element and k_B is Boltzmann's constant. However, the value of the Lorentz constant depends on the material and temperature in actual experiments. The value of the Lorentz constant for aluminum alloy is $\sim 2.1 \times 10^{-8} \text{ V}^2 \text{ K}^2$ [53].

For the phonon thermal conductivity, it is more difficult to measure directly. Some studies use the simulation method to calculate the phonon thermal conductivity in non-metallic materials [54,55]. In general, the phonon thermal conductivity is a function of the temperature. In pure aluminum, the phonon thermal conductivity is shown as follows [56]:

$$\lambda_p = \left(\frac{T}{1700} + \frac{50}{T^2} \right)^{-1} \quad (7)$$

In aluminum alloys, the phonon thermal conductivity is expressed via the Wiedemann–Franz law [57]:

$$\lambda = \frac{L_0 T}{\rho} + B T^n \quad (8)$$

$$\rho = \frac{1}{\sigma} \quad (9)$$

where ρ is the electrical resistivity of aluminum alloys, B is a constant, and the range of the parameter n is from $-1 \sim 0$.

It occupies only a small ratio of $\sim 2.4\%$ in the total thermal conductivity of aluminum [58]. In aluminum alloys, the temperature slightly affects the phonon thermal conductivity according to a previous study [57]. Accordingly, the phonon thermal conductivity is often seen as a constant by fitting the linear Wiedemann–Franz law in aluminum alloys.

$$\lambda = L_0 T \sigma + C \quad (10)$$

In the literature, C values are given from $10.5 \sim 12.6 \text{ W m}^{-1} \text{ K}^{-1}$ [53]. However, in metals, although the ratio of the phonon thermal conductivity is quite small, it is a part of the thermal conductivity of aluminum alloys. Moreover, the phonon thermal conductivity in pure aluminum is $\sim 6 \text{ W m}^{-1} \text{ K}^{-1}$ as calculated by Formula (7) at 298 K. However, the fitting phonon thermal conductivity of aluminum alloys is much higher than this value, and different references about different alloys have different values of the phonon thermal conductivity. This shows that the phonon thermal conductivity also varies with alloy compositions. Thus, more in-depth studies about the relationship between the phonon thermal conductivity and alloy compositions in aluminum alloys are still needed.

Actual aluminum alloys often consist of an Al lattice with impurities of different states introduced by alloying elements. Therefore, the real heat transfer of aluminum alloys is often affected by them. Then, the scattering process emerges to hinder the heat transfer. electrons cause electron–electron scattering, electron–phonon scattering, and electron–impurity scattering. Phonons cause phonon–phonon scattering (U-process) and phonon–impurity scattering [58,59]. Because of the dominant heat transfer role of free electrons, the previous three scattering processes involving electrons are often considered in aluminum alloys. A schematic of the main scattering patterns is shown in Figure 5. Compared to the two other intrinsic scattering mechanisms, electron–impurity scattering is of greater importance and concern in alloys. Regarding reducing the electron–impurity scattering, many investigators tried to control the impurity in die-cast aluminum alloys to improve their thermal conductivity. Experiments and theoretical results are discussed in detail in following sections.

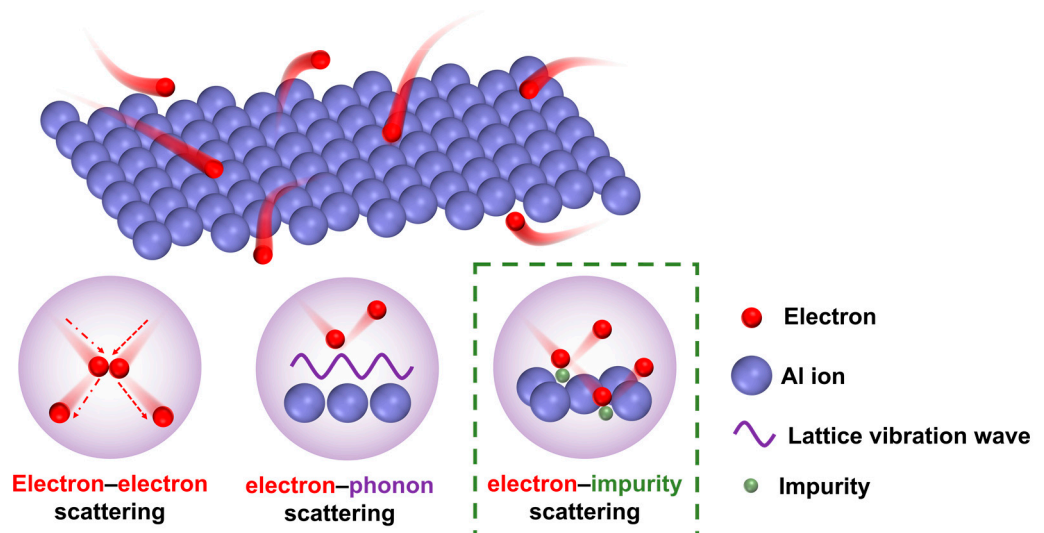


Figure 5. Electron scattering patterns in an aluminum alloy.

3. Die-Cast Aluminum Alloys for Thermal Conductivity

In die-cast aluminum alloys, there are many species with different major alloying elements like Si, Mg, Cu, etc. Affected by alloying elements, different kinds of aluminum

alloys have distinct thermal conductivities. According to Matthiessen's rule [60], the electrical resistivity (thermal conductivity) is affected by the lattice, solid solution, precipitate, grain boundaries, dislocations, vacancies, etc., which is written as follows:

$$\rho = \rho_p(T) + \sum_i \rho_s^i c_s^i + \sum_i \rho_p^i c_p^i + \rho_g + \rho_d + \rho_v \quad (11)$$

where the $\rho_p(T)$ is the basic electrical resistivity of the pure Al matrix which is a function of temperature T , ρ_s^i is the resultant electrical resistivity increase when the element i increases by 1 wt.% in the Al solid solution, ρ_p^i is the resultant electrical resistivity increase when the element i increases by 1 wt.% as the precipitate, c_s^i is the content of the element i in the Al solid solution, c_p^i is the content of the element i as the precipitate. ρ_g is the electrical resistivity due to grain boundaries, ρ_d is the electrical resistivity due to dislocations, and ρ_v is the electrical resistivity due to vacancies. For alloying elements, the content of the element in the Al solid solution and the secondary phase, and the electrical resistivity increase caused by the increase of per wt.% of the element in the Al solid solution and the secondary phase determine the electrical resistivity.

Therefore, $\sum_i \rho_s^i c_s^i$ and $\sum_i \rho_p^i c_p^i$ are the main factors. In a previous study [59], the quantitative values of the effect extents of different additions of elements on electrical resistivity in aluminum (ρ_s^i, ρ_p^i) are summarized in Table 2. From Table 2, the harmful effect of a solid solution containing alloying elements on electrical resistivity (thermal conductivity) is much higher (mostly over 10 times) than that of the precipitate state according to the value of ρ_s^i / ρ_p^i .

Table 2. Effect of alloying elements in solid solutions and precipitates on electrical resistivity of aluminum (ordered by the maximum solubility of elements in α -Al) [61].

Alloying Element	Maximum Solubility in α -Al (wt.%)	Increase in Electrical Resistivity in Solid Solutions (ρ_s^i ($\mu\Omega$ cm wt.% ⁻¹))	Increase in Electrical Resistivity in Precipitates (ρ_p^i ($\mu\Omega$ cm wt.% ⁻¹))	ρ_s^i / ρ_p^i
Zn	82.8	0.094	0.023	4.09
Mg	14.9	0.54	0.22	2.45
Cu	5.65	0.344	0.03	11.47
Li	4	3.31	0.68	4.87
Mn	1.82	2.94	0.34	8.65
Si	1.65	1.02	0.088	11.59
Ti	1	2.88	0.12	24
Cr	0.77	4.00	0.18	22.22
V	0.6	3.58	0.28	12.79
Zr	0.28	1.74	0.044	39.55
Fe	0.05	2.56	0.058	44.14
Ni	0.05	0.81	0.061	13.28

Note: The values of ρ_p^i are limited to twice the maximum solubility of elements in α -Al except Mg (limited to ~10 wt.%) and Zn (limited to ~20 wt.%).

Furthermore, the basic regularity of the influence trend of alloying elements on the thermal conductivity and electrical conductivity of aluminum has been also investigated using theoretical and experimental methods [58,62–64], shown in Figure 6. Among several common elements, the orders of the detrimental effect on electrical conductivity and thermal conductivity in Figure 6a,b are Zn < Cu < Si < Mg < Zr < Ti < V < Mn < Cr and Zn < Cu < Mg < Si (Si < Mg in Figure 6c) < Zr < Ti < Mn < V < Cr, respectively. Reference [63] also revealed that rare elements had a small effect on the electrical conductivity of aluminum. Obviously, the element Si influences the thermal conductivity to a reduced extent compared with Zr, Ti, V, Mn, and Cr and also has excellent castability and acceptable strength for die-cast aluminum alloys compared to elements before Si [65]. Thus, Al–Si alloys are the most common system for die-cast heat dissipation components. In addition, in order to

avoid the primary phase of the secondary element reducing thermal conductivity severely, the general composition of die-cast Al alloys with high thermal conductivity should be on the hypoeutectic side.

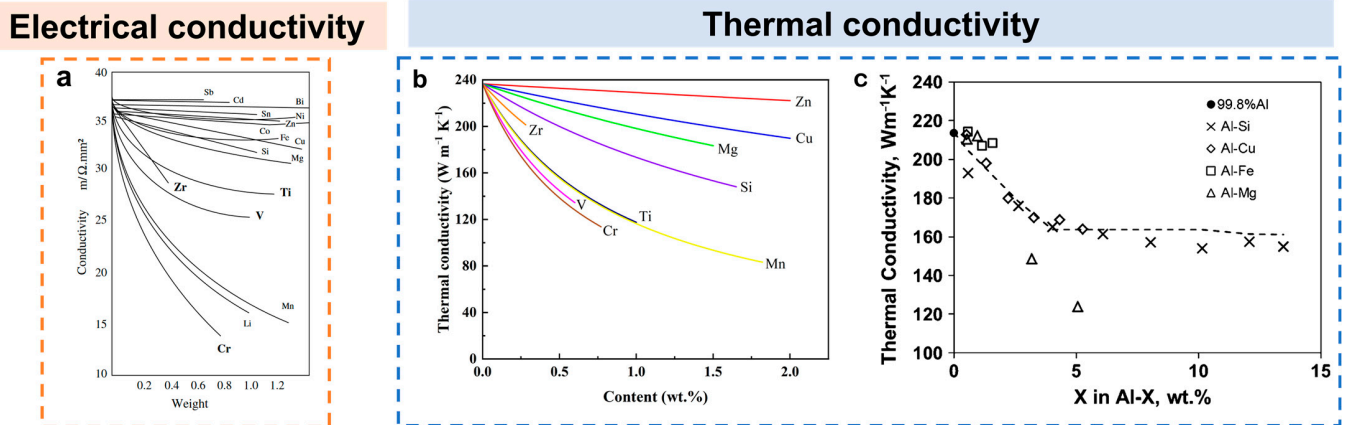


Figure 6. The effect of alloying elements on (a) electrical conductivity (reprinted with permission from ref. [62], 2006, Elsevier) and thermal conductivity using (b) theoretical method (reprinted with permission from ref. [58], 2023, Springer) and (c) experimental method of aluminum alloys (reprinted with permission from ref. [64], 2015, Springer).

3.1. Al–Si Alloys

Generally, the Si content is often near-hypoeutectic in high-strength and high-ductility die-cast Al–Si alloys, ranging from 9 wt.% to 12 wt.%, such as Silafont[®]-36 (AlSi10MnMg), Silafont[®]-38 (AlSi9MnMgZn), Castasil[®]-37 (AlSi9MnMoZr), ADC12 (AlSi11Cu3), and A380 (AlSi9Cu3) [66,67]. However, the thermal conductivity of these alloys only ranges from 90 to 130 $\text{W m}^{-1} \text{K}^{-1}$ in Table 1. For example, Celal Cingi et al. [68] found that the A380 die-cast alloy exhibited a thermal conductivity of $\sim 115 \text{ W m}^{-1} \text{K}^{-1}$ and a hardness of $\sim 83 \text{ HV}$. The microstructure consisted of primary α -Al grains with $\sim 10 \mu\text{m}$ and a large area fraction of eutectics enriching Si and Cu. These eutectics played an important role in improving the hardness and reducing the thermal conductivity. Furthermore, die-cast alloys developed by Rheinfelden [25], Silafont[®]-36, Silafont[®]-38, and Castasil[®]-37, contain a large area fraction of eutectic silicon in their microstructures. Additionally, Jiao et al. [69] investigated the Silafont[®]-36 die-cast alloy and tested concentrations of elements in primary α -Al. The maximum Si, Mg, and Mn contents were 4.26 wt.%, 0.39 wt.%, and 0.20 wt.%, respectively, higher than the solubility at room temperature. This means that in die-casting processes with a high solidification rate, the α -Al grains are supersaturated. Therefore, the main reasons for the low thermal conductivity of these alloys are as follows, as shown in Figure 7. On the one hand, to ensure high strength, these alloys often contain high contents of Si, Mg, Cu, Mn, etc. [70]. The maximum solubility values of Si, Mg, Cu, and Mn in aluminum are 1.65 wt.%, 14.9 wt.%, 5.67 wt.%, and 1.82 wt.%, which are not very low. However, the detrimental effect of transition metals like Mn is quite serious as shown in Figure 6 and Table 2. Therefore, there are plenty of solid solutions containing alloying elements (Si, Mg, Cu, Mn, etc.) in the alloy and the solubility in the substrate of die casting is higher than that of the equilibrium state. These solid solutions increase the scattering of electrons [71]. On the other hand, high contents of elements such as Si and Cu result in a large volume fraction of eutectic particles in the die-cast alloy, which causes impurity scattering from precipitates [72,73]. Therefore, to address these problems, some methods are employed to obtain die-cast Al–Si alloys with higher thermal conductivity. Firstly, one method is to reduce Si and other elements' contents to mitigate the detrimental effect of the major elements. Then, adding minor elements into Al–Si alloys to optimize the microstructure to improve the thermal conductivity is also a key method. The method can be divided

into two parts, including reducing the solute concentration of trace elements in the solid solution and modifying the eutectic particles.

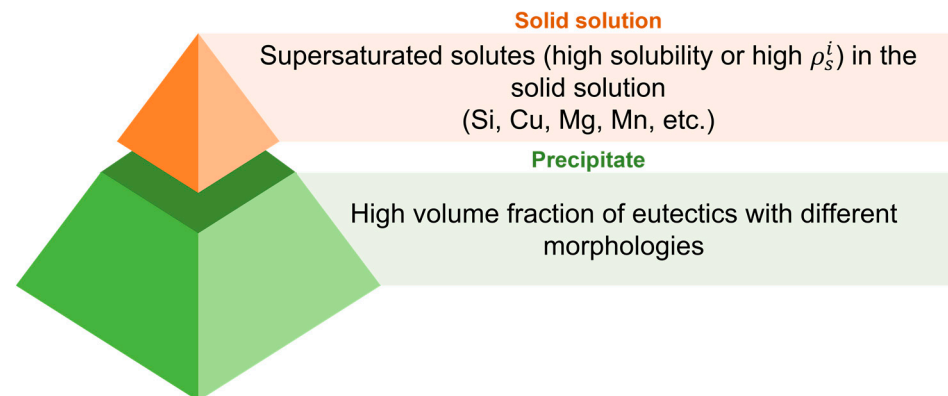


Figure 7. Problems of traditional Al-Si die-cast alloys.

3.1.1. Reducing the Content of Major Elements

For the first method, many studies firstly concentrate on reducing Si and other elements' contents. Rheinfelden company [25] developed Castasil[®]-21 alloy (AlSi9Sr) by removing other alloying elements like Cu, Mg, and Mn as well as maintaining a Si content of 9% and a Fe content within 0.5~0.7%. In the as-cast state, the die-cast alloy obtains a yield strength, ultimate tensile strength, and elongation of 90~100 MPa, 200~230 MPa, and 6~9%, respectively, which are lower than those of other high-strength die-cast Al-Si alloys. However, the thermal conductivity of the die-cast alloy is over $160 \text{ W m}^{-1} \text{ K}^{-1}$. To increase thermal conductivity, the alloy should be annealed at $250 \text{ }^\circ\text{C}$ ~ $350 \text{ }^\circ\text{C}$. Considering the high Si content, some studies aimed to reduce the Si content to enhance thermal conductivity. Qi et al. [74] studied Al-8Si heat dissipation die casting containing Fe without involvement of other elements and there were plenty of eutectic Si phases and needle-like β -Al₅FeSi eutectic phases in the microstructure as shown in Figure 8a. Thermal conductivity of the casting reached $156 \text{ W m}^{-1} \text{ K}^{-1}$ and the tensile strength was 211 MPa. To obtain higher strength, researchers added some other elements based on Al-(6~8)Si alloys. M. Payandeh et al. [75] considered using ~2 wt.% Cu and below 1 wt.% Zn in Al-6Si die-cast alloys. In Figure 8b, Al₂Cu particles in the alloy improved the hardness to 75 HV and maintained thermal conductivity within 140 ~ $150 \text{ W m}^{-1} \text{ K}^{-1}$ for the die-cast alloy. Furthermore, except Zn, Jae-Cheol Jang et al. [76] added elements Ni and Cu with different contents into Al-6Si die-cast alloys. The strength increased by over 300 MPa mainly due to the solid solution strengthening from element Cu. However, the thermal conductivity decreased to 120 ~ $130 \text{ W m}^{-1} \text{ K}^{-1}$, caused by high Cu content in the substrate [77–79]. In addition, L. Kumar et al. [80] designed three die-cast alloys with Si contents from 6~8 wt.% and Mg or Cu with contents over 1 wt.% to strengthen the alloy. The thermal conductivity and tensile strength values of three alloys were $160.3 \text{ W m}^{-1} \text{ K}^{-1}$, $153.0 \text{ W m}^{-1} \text{ K}^{-1}$, and $146.0 \text{ W m}^{-1} \text{ K}^{-1}$ and 307 MPa, 331 MPa, and 350 MPa as shown in Figure 8c. The study also confirmed that secondary phases (Al₅Cu₂Mg₈Si₆, Al₇Cu₂M, and β -AlFeSi phases) strongly increased the mechanical properties and the thermal conductivities of the three samples were negatively correlated with the fraction of these secondary phases. Cr and Ti were also added into the Al-7Si-3Mg die-cast alloy [81]. The tensile strength improved to over 340 MPa, but thermal conductivity decreased below $140 \text{ W m}^{-1} \text{ K}^{-1}$ because of the strongly detrimental effect of Cr and Ti (Table 2). These studies successfully provide a strategy that, if the contents of strengthening elements are suitable, using a low-Si die-cast alloy with these strengthening alloying elements can achieve a similar strength to that of high-strength alloys and a higher thermal conductivity. According to the above results, low Si (around 6 wt.%) and suitable Cu contents for strengthening are preferred to synergistically improve comprehensive properties compared to traditional die-cast Al-Si alloys

because the low ρ_s^i value ($0.344 \mu\Omega \text{ cm wt.\%}^{-1}$) (Table 2) reduces the electron scattering in the solid solutions.

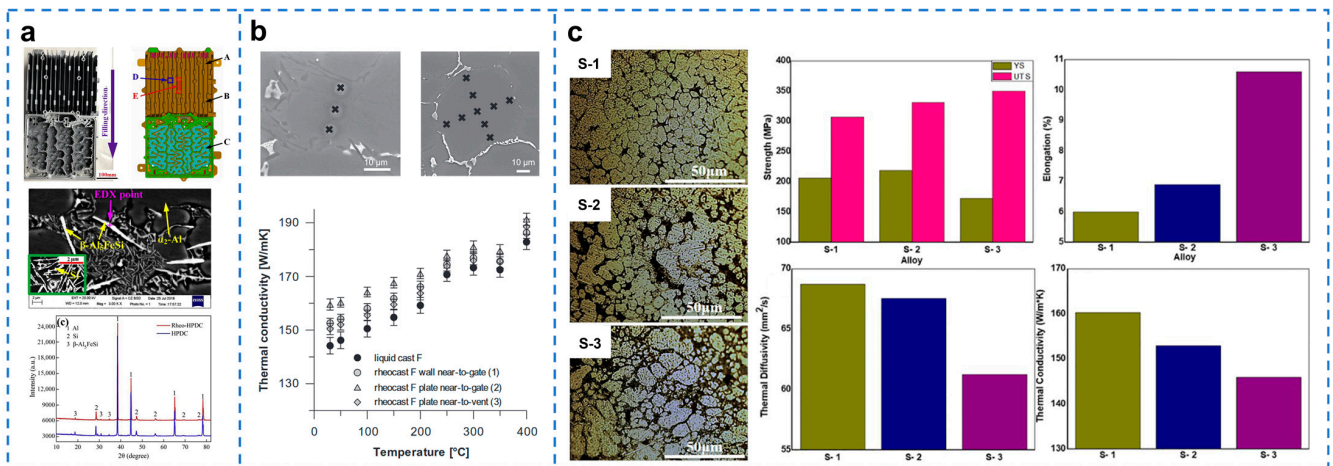


Figure 8. Microstructure and properties of different Al-Si die-cast alloys with low Si contents: (a) Al-8Si (reprinted with permission from ref. [74], 2018, Elsevier), (b) Al-6Si with Cu and Zn (reprinted with permission from ref. [75], 2016, Springer), (c) Al-(6-8)Si with Cu or Mg (reprinted with permission from ref. [80], 2022, Elsevier).

Meanwhile, some studies [82,83] focus on Al-Si die-cast alloys with ultra-low Si content within 1~2 wt.%. Although these alloys can achieve a high thermal conductivity of over $180 \text{ W m}^{-1} \text{ K}^{-1}$, the low elemental contents make the ultimate tensile strength below 150 MPa and significantly reduce the fluidity compared to ADC12. Y. H. Cho et al. [84] studied the effect of Ni on Al-2Si alloy and increased the cooling rate to approximate the real die-casting process. At the high cooling rate, the thermal conductivity of Al-2Si-xNi could be within $170\sim 190 \text{ W m}^{-1} \text{ K}^{-1}$. With the increase in Ni contents, the Al_3Ni phase was formed to decrease thermal conductivity. Notably, the increase in Ni content could decrease the Si solutes in the matrix, thereby mitigating the decrease in thermal conductivity. Regarding the fluidity, because of the ($\alpha\text{-Al} + \text{Al}_3\text{Ni} + \text{Si}$) ternary eutectic point (Ni content is $\sim 0.47 \text{ wt.\%}$) with a low solidification range as shown in Figure 9, the fluidity length of Al-2Si-0.5Ni increased at the top. However, it still only achieved 80% of the fluidity of ADC12 alloy. These three studies discussed above uncover a big problem of ultra-low Si alloys in that they cannot obtain enough castability and strength like commercial Al alloys and pose a challenge for real die-cast production, although having great thermal conductivity.

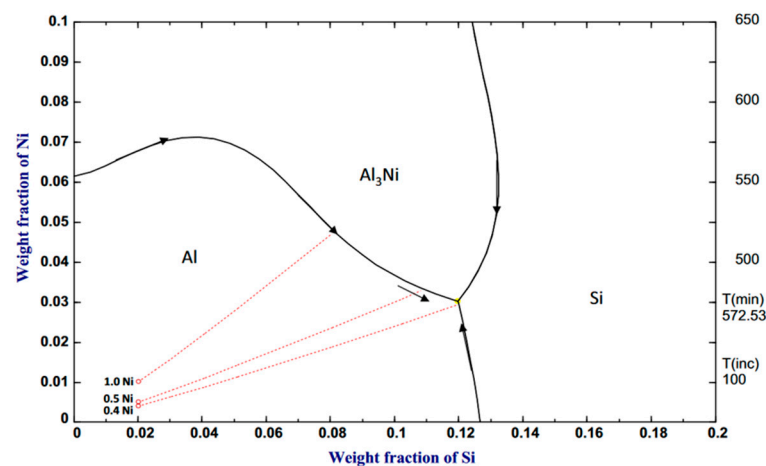


Figure 9. The ternary eutectic point of the Al-Si-Ni system (reprinted with permission from ref. [84], 2015, Springer).

3.1.2. Reducing the Solute Concentration of Trace Elements in Solid Solutions

Regarding reducing the solute concentrations of trace elements in the solid solution, trace solutes in the solid solution include alloying elements and impurity elements. Lumley et al. [61] found that sometimes an increase in Mn content could increase the thermal conductivity by $\sim 10 \text{ W m}^{-1} \text{ K}^{-1}$ of Al–Si die-cast alloys containing Fe and Mn as shown in Figure 10a, which was contrary to the common sense related to the high ρ_s^i of Mn. This was because the primary phase $\text{Al}_{15}(\text{Mn}, \text{Fe})_3\text{Si}_2$ in the alloy, which was one of the iron-rich phases in the Al–Si alloys [85–87], would precipitate from the liquid before primary α -Al in the as-cast alloy. It nearly consumed most Mn to form block-like compounds combined with Fe and only a very small number of solutes were in the matrix. Moreover, for reducing impurity elements, boron treatment is one of the common methods to improve the thermal conductivity and electrical conductivity of aluminum alloys [88–90]. In aluminum alloys, there are plenty of transition metals like Ti, Zr, Cr, V, etc. Although their contents are quite small, they can cause large lattice distortion in Al substrates [88]. This can lead to the high ρ_s^i value shown in Table 2 and can be severely harmful to electrical and thermal conductivity. In general, boron forms AlB_2 with Al. However, considering elements Ti, Zr, Cr, and V, because the Gibbs free energy of these borides is lower than that of AlB_2 (TiB_2 , ZrB_2 , VB_2 , CrB_2) [91], these atoms react with the borides to replace Al atoms through diffusion [71,92–94]. Accordingly, various kinds of precipitate-state borides with transition metals are formed. Due to the high atomic order of transition metals, borides containing these metals have a higher density than aluminum. As a result, they tend to settle at the bottom of the furnace, carrying solutes with them, as depicted in Figure 10b. Thus, the solutes in the solid solution decrease, which increases the average path of electrons, and the electrical and thermal conductivity are improved. Yang et al. [95] added a trace amount of B (<0.05 wt.%) to ADC12 alloy. Electrical conductivity increased from 18.48 MS m^{-1} to 19.22 MS m^{-1} after adding 0.02 wt.% B, as shown in Figure 10c. Moreover, the decrease in solutes was confirmed by the variation in the lattice constant determined from XRD peaks in Figure 10c. Veijo Rauta et al. [96] also investigated the effect of B on Anticorodal[®]-04 alloy (AlSi0.5Mg) for HPDC. Similar results showed that the thermal conductivity of Anticorodal[®]-04 alloy after boron treatment improved by about 3.8–4.4% with a decrease in transition metal elements. Unfortunately, the results above are both alloys for die casting but used the gravity-casting process. However, there is still limited research on the thermal conductivity variation of die-cast samples after boron treatment.

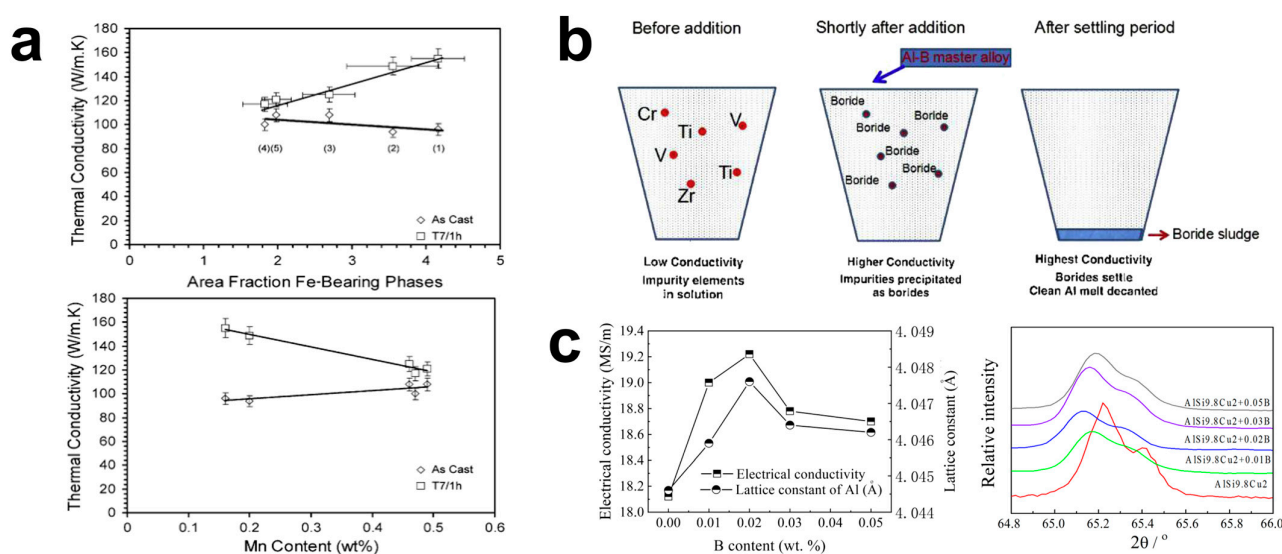


Figure 10. (a) Effect of Mn on thermal conductivity of the die-cast Al–Si alloy (reprinted with permission from ref. [61], 2013, Springer). (b) The purification process of boron treatment (reprinted with permission from ref. [91], 2018, Elsevier) and (c) the effect of boron on the thermal conductivity of ADC12 alloy (reprinted ref. [95]).

3.1.3. Modification of Eutectic Particles

For the modification of the eutectic particles (i.e., eutectic silicon particles in Al–Si alloys), the particle morphology is changed from a plate shape to a fibrous shape [97]. The most commonly used element for modifying Si is Sr. Other elements like Ca, Sb, Na, and rare earth (RE) elements were also reported [98]. The modification mechanisms of eutectic silicon mainly include the impurity-induced twinning growth mechanism [99] and the twinning plane re-entrant edge mechanism [100]. The evolution of eutectic silicon morphology increases the free path of electrons by reducing the barriers imposed by secondary phases with low thermal conductivity and by mitigating lattice distortions in α -Al grains as shown in Figure 11a,b [24,51]. Wen et al. [51] compared the thermal conductivities of gravity-cast Al–7Si alloys modified with various trace elements (Sr, RE, Sb). The alloy treated with strontium exhibited fully modified eutectic silicon, obtaining the greatest improvement in thermal conductivity compared to other elements. Based on the excellent modification of Sr, in die-cast Al–Si alloys, various composite modifications of eutectic silicon that include strontium have been developed. Hiromi Nagaumi et al. [101] investigated the effect of Sr and Ca on the thermal conductivity of a eutectic Al–Si alloy. The thermal conductivity was the highest with absolute modification when the addition of Ca and Sr were both 0.05 wt.%. Then, they developed a fully modified Al12Si–HTC alloy using both Sr and Ca to produce a die-cast communication enclosure with a thermal conductivity of up to $160 \text{ W m}^{-1} \text{ K}^{-1}$. The simulation results indicated that the optimized alloy had an improvement of 41.6% in thermal conductivity compared to Al12Si. Additionally, Liu et al. [102,103] incorporated Sr and Ce, Sr, and Er into AlSi10MnMg alloy to improve thermal conductivity and mechanical properties simultaneously. The addition of Ce to achieve the best comprehensive properties was significantly smaller than that of Er. A study [104] demonstrated that rare earth elements could also react with Si to decrease the solubility of Si in the solid solution. However, its effect was smaller than that of the modification and has not been given much attention. Moreover, a study [105] reported that with the increase in cooling rate, the eutectic silicon was also modified without other elements, which indicated direct modification from the die-casting process with a high solidification rate.

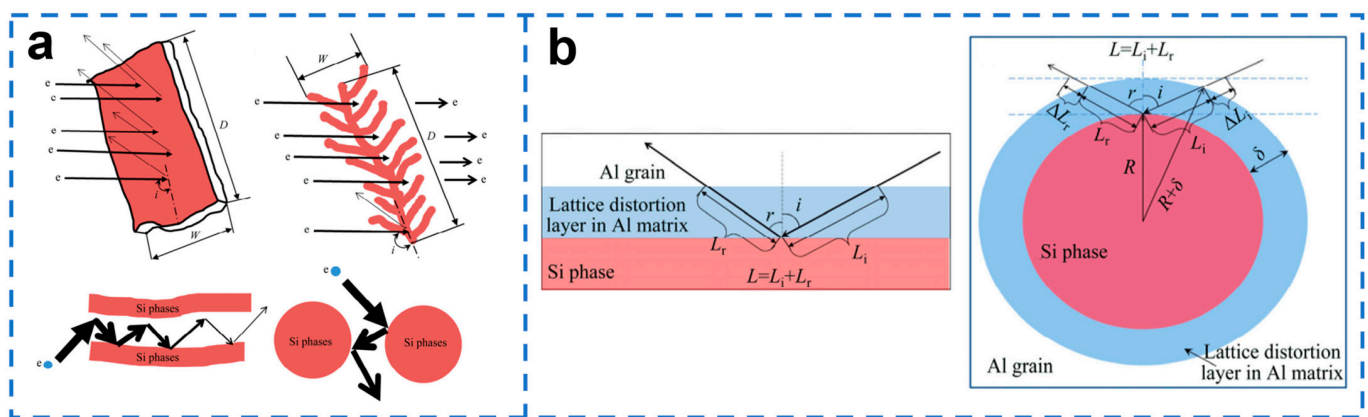


Figure 11. (a,b) Mechanism of improving thermal conductivity by modifying the eutectic Si (reprinted with permission from ref. [24], 2020, Springer).

However, the strategies mentioned above have their disadvantages. The first strategy requires decreasing the Si content, which compromises the casting ability of Al–Si alloys at the same time [106]. Moreover, the improvement in thermal conductivity achieved by adding trace elements is also limited. Neither of these methods can meet the higher requirements for thermal conductivity due to the major element Si having a high eutectic point. Accordingly, many researchers have begun to focus on other aluminum alloys that do not contain Si to develop new die-cast alloys with high thermal conductivity.

3.2. Silicon-Free Aluminum Alloys

3.2.1. Al–Ni Alloys

In Table 2, we can see that Ni has low solubility in Al (~0.05 wt.%) and that the value of ρ_s^i ($0.81 \mu\Omega \text{ cm wt.\%}^{-1}$) is quite small. The element mainly exists as the secondary phase in the alloy. This indicates that Ni has a minimal detrimental effect on thermal conductivity. Moreover, the eutectic point is ~5.7 wt.% [107], which is much lower than that of Al–Si alloys. This means that the Ni content is much lower than Si in the near-eutectic-composition alloys. Furthermore, the morphology of the eutectic Al_3Ni in the Al–Ni alloys is fibrous [108], which allows for easy electron transport. Therefore, Ni becomes a potential element for developing high-thermal-conductivity die-cast alloys. Tesla Inc. [109] developed a near-hypoeutectic die-cast Al–5.3Ni–0.35Fe–0.03Ti alloy with an electrical conductivity of 50% IACS and a yield strength of 90 MPa for automobile parts in 2018. In addition, for microstructure optimization, Yb [110] was also employed to modify eutectic Al_3Ni phases and improve the thermal conductivity and mechanical properties of an Al–5Ni gravity-cast alloy. However, the high cost of Ni also restricted the application of Al–Ni alloys. Nikkei MC Aluminum Co. [111] developed the DX26 die-cast alloy (Al–2Ni–Fe) with a thermal conductivity of $190 \text{ W m}^{-1} \text{ K}^{-1}$ by reducing Ni content. However, the concentration is so far away from the eutectic point that the castability becomes a possible issue for applications. In conclusion, because of the trade-off between cost and castability, implementing this system for high-thermal-conductivity applications is still challenging.

3.2.2. Al–Fe(–Ni) Alloys

To solve the problem regarding Al–Ni alloys and search for an element with a lower eutectic point to ensure castability and cost, Fe draws attention to developers because of the similar low solubility (~0.05 wt.%) in the Al matrix. Most Fe combines with Al to form a plate-like $\text{Al}_{13}\text{Fe}_4$ phase [112]. The eutectic point of Fe is ~1.75 wt.%, which is much lower than that in Al–Ni and Al–Si binary systems [113]. This indicates that an Al–Fe system can be used to obtain ultra-high thermal conductivity because of the low elemental contents. Meanwhile, Fe is crucial for the die-casting process due to its soldering resistance characteristic [59]. Nikkei MC Aluminum Co. [111] also developed the DX01 die-cast alloy (Al–Fe) with a thermal conductivity of over $200 \text{ W m}^{-1} \text{ K}^{-1}$. However, the yield strength is only 57 MPa, which is similar to that of pure Al. Ki-Tae Kim et al. [114] added Zn, which has a low ρ_s^i value ($0.094 \mu\Omega \text{ cm wt.\%}^{-1}$), with Fe into a die-cast Al alloy. When the Zn (1.91 wt.%) and Mg (0.17 wt.%) contents were low, thermal conductivity was over $190 \text{ W m}^{-1} \text{ K}^{-1}$ and tensile strength was slightly above 100 MPa. Some studies under the gravity-cast state also discussed ways toward microstructure optimization of Al–Fe alloys. La [115], Ce [116], and Co [117] were used to modify the eutectic $\text{Al}_{13}\text{Fe}_4$ phase from a plate-like shape to a spotted shape and improved the mechanical properties and thermal conductivity. However, there is no similar study about die-cast Al–Fe alloys and the positive modification effects on the microstructure and thermal conductivity of die-cast Al–Fe alloys cannot be verified. Considering the strengthening effect and minimal adverse impact on the thermal conductivity of Ni, a new ternary Al–Fe–Ni alloy was designed. The eutectic composition Al–1.75Fe–1.25Ni was used to maintain a low solidification range [118]. In the Al–Fe–Ni ternary alloy, a new fibrous eutectic Al_9NiFe phase, which was similar to Al_3Ni , was formed [119,120]. The thermal conductivity of the gravity-cast Al–1.75Fe–1.25Ni alloy could be over $200 \text{ W m}^{-1} \text{ K}^{-1}$ [121]. Luo et al. [122] studied the effects of several elements including Co, Ce, and Yb on the thermal conductivity of the eutectic Al–1.75Fe–1.25Ni gravity-cast alloy. Only Yb could refine the (α -Al + Al_9NiFe) eutectic cell and improve the strength and thermal conductivity simultaneously.

In summary, many silicon-free HPDC aluminum alloys have been developed for new-generation heat dissipation applications with high thermal conductivity as shown in Table 3. However, although some studies were carried out on gravity-cast aluminum alloys, there are few systematical and deep studies about the microstructure and thermal conductivity of die-cast Al–Ni/Al–Fe(–Ni) aluminum alloys like the Al–Si series. Moreover,

the low alloy compositions allow these alloys to improve mechanical properties while maintaining high thermal conductivity and castability to break the trade-off between strength, castability, and thermal conductivity by microstructure optimization. Furthermore, for the practical application of large-size products, die castings produced by these alloys should be optimized and adjusted combined with several processing parameters.

Table 3. Physical properties and yield strength of silicon-free (Al–Ni, Al–Fe, Al–Fe–Ni) die-cast (DC)/gravity-cast (GC) aluminum alloys.

Alloy	Process	Temper	Electrical Conductivity (% IACS)	Thermal Conductivity ($\text{W m}^{-1} \text{K}^{-1}$)	Yield Strength (MPa)	Ref.
Al–5.3Ni–0.35Fe–0.03Ti	DC	F	50	-	90	[109]
DX01	DC	F	51	205	57	[111]
DX02	DC	F	51	200	64	[111]
DX26	DC	F	48	190	68	[111]
Al–1.75Fe–1.25Ni	GC	F	52	207	-	[121]

4. Effect of Die-Cast Processing on Thermal Conductivity in Die-Cast Aluminum Alloys

4.1. Processing Parameters of High-Pressure Die Casting

The HPDC process affects the microstructure including primary α -Al, eutectics, and porosity in die-cast aluminum alloys, which also significantly determines the thermal conductivity of die-cast aluminum alloys. The main processing parameters include slow-shot speed, fast-shot speed, intensification pressure, and vacuum [17,23,67,69]. J.K. Chen et al. [123] studied different shot speeds and intensification pressures and their effects on the porosity and thermal conductivity of die-cast Al–10Si alloy. With an increase in die-cast speeds and a decrease in pressure, the volume fraction of porosity increased. Because of the low thermal conductivity of the air, more porosities caused lower thermal conductivity of die-cast Al–10Si alloys as shown in Figure 12a. From the calculation, per percentage of porosity brought a $\sim 4.7 \text{ W m}^{-1} \text{ K}^{-1}$ decrease in thermal conductivity. Hu et al. [124] compared the thermal conductivity of a die-cast Al–12Si alloy with different vacuum levels. When the vacuum level increased from 275 mbar to 72 mbar, the volume fraction of pores decreased from 0.152% to 0.046%, and thermal conductivity increased 3.84% as shown in Figure 12b,c. However, these studies only considered the effect of porosity variation on the thermal conductivity of die-cast aluminum alloys. Different processing parameters also influence other parts of microstructure and these effects have not been considered yet. Liu et al. [125] tried to control the fraction of ESCs in a die-cast Al–Mg–Si alloy using a new shot sleeve with a ceramic layer, thus changing the solute concentrations in the Al matrix and improving the thermal conductivity as shown in Figure 12d,e.

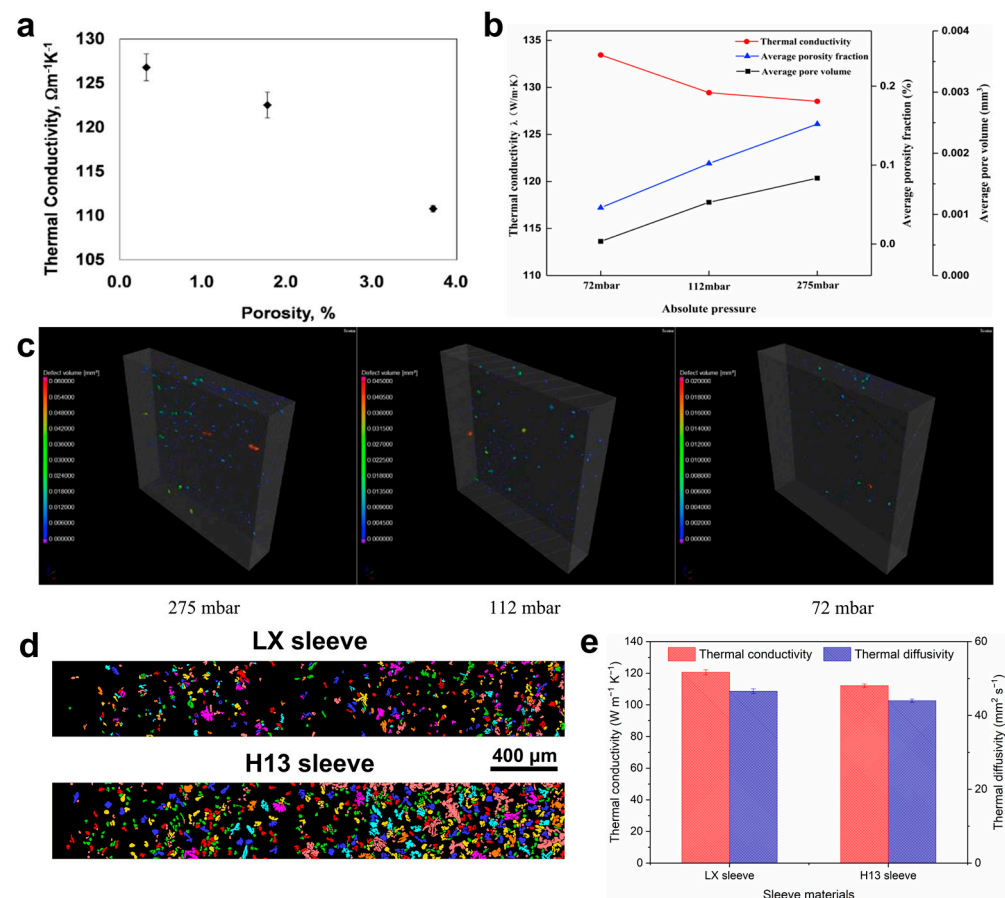


Figure 12. (a) Variation in thermal conductivity under different fractions of porosity caused by processing parameters (reprinted with permission from ref. [123], 2017, Elsevier). (b) Thermal conductivity and corresponding (c) porosity distribution under different vacuum levels (reprinted with permission from ref. [124], 2020, Elsevier). (d) Distribution of ESCs and (e) thermal conductivity of die-cast alloys under different shot sleeves (reprinted with permission from ref. [125], 2022, Elsevier).

4.2. Rheological High-Pressure Die Casting

Apart from the traditional HPDC technique, the rheological die-casting process is also used in fabricating aluminum die castings. This technique includes the use of a slurry maker in conjunction with a traditional die-cast machine [126]. In the slurry maker, under the stirring of a screw, the melt has a high shearing rate and strong turbulence, and then the melt becomes a high-viscosity semisolid slurry with spherical particles under heat transfer. Then, the slurry is poured into the shot sleeve and the general die-casting process is performed. By incorporating the slurry maker process, die castings with lower porosity fractions and better mechanical properties can be obtained [127,128]. These advantages have led to increased interest in the rheological die-casting process for manufacturing high-quality die castings. Through the rheological die-casting process, Al–Si die casting with a higher thermal conductivity than traditional die casting was prepared because of the lower Si concentration in the Al matrix [75]. Qi et al. [36,129] employed an air compressor in the rheological die-casting process (ACSR Rheo-HPDC process) to help lower the temperature of the melt and produced the semisolid slurry shown in Figure 13. By adjusting the proper airflow, the Al–Si die-cast alloy could achieve an improvement in thermal conductivity from $167 \text{ W m}^{-1} \text{ K}^{-1}$ to $184 \text{ W m}^{-1} \text{ K}^{-1}$ and a higher elongation of over 10%. The improvement of thermal conductivity was attributed to an increase in the nucleation rate due to the air cooling the melt, which refined the secondary phases in the alloy and increased the free path of electrons for the heat transfer.

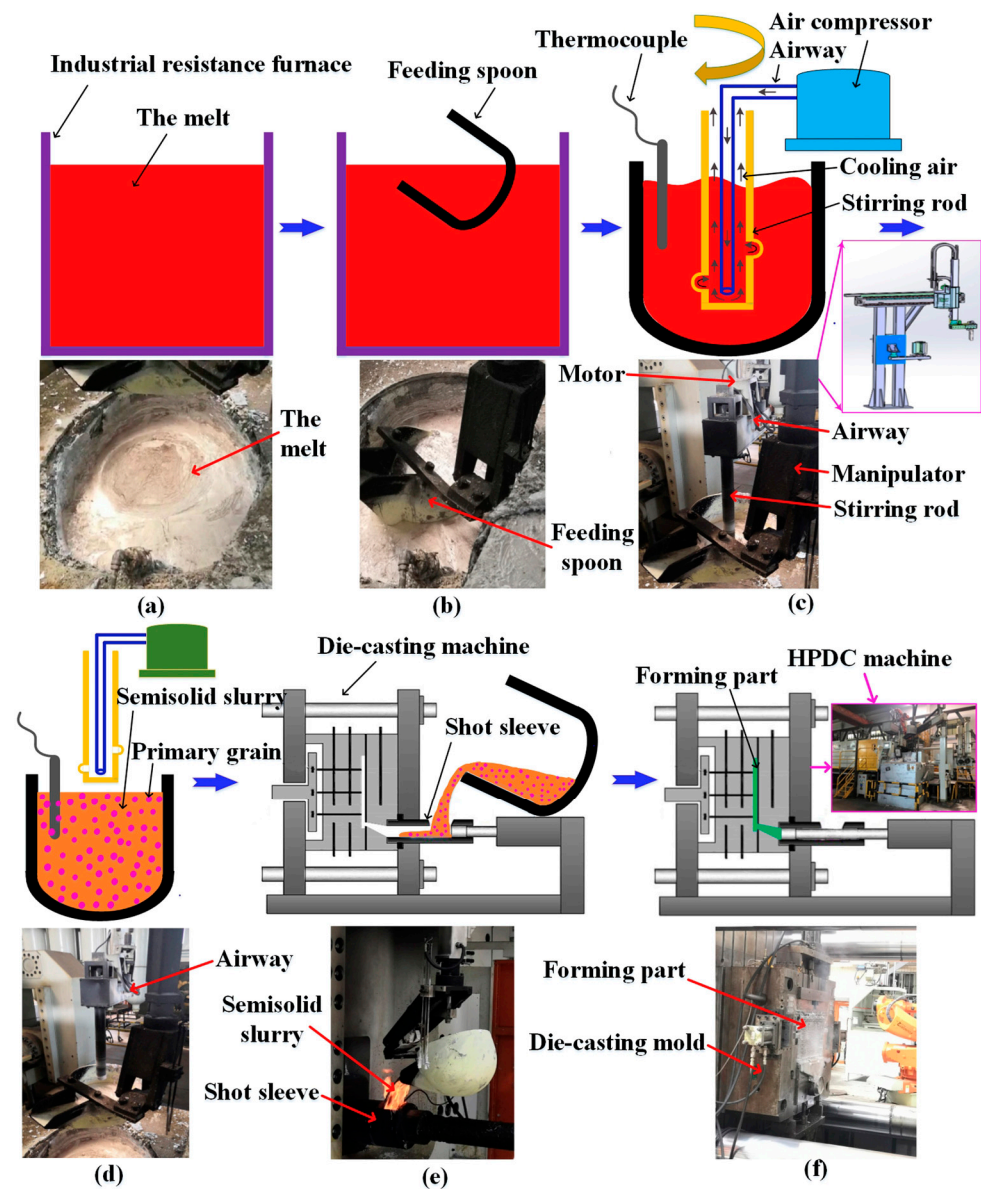


Figure 13. The schematic diagrams of the ACSR Rheo-HPDC process (reprinted with permission from ref. [36], 2022, Elsevier).

Recently, some commercial software in the market was used to simulate the heat conduction of filling and solidification during the die-casting process successfully [130]. Assisted by MAGMASOFT® and ANSYS Fluent®, K. Arunkumar et al. [131] developed a coupled simulation strategy to determine accurate heat transfer coefficients of the die-cooling channel and optimized the key parameters in the solidification of the die casting. Furthermore, ANSYS Fluent® was also used to obtain the interface heat transfer coefficients during the die-casting process and clarified the influence factors (injection pressure, injection second phase velocity, casting temperature, vacuum, etc.) had on the interface heat transfer coefficients combined with experimental and numerical results [132]. Furthermore, simulations of the temperature field distribution in the mold during the melt filling process have also been studied by software like FLOW-3D CAST™, ProCAST, and MAGMASOFT® [133–136]. These excellent works have guided optimization of the parameters of the HPDC process in industry.

From the results above, processing parameters of HPDC significantly influence the thermal conductivity of Al alloys. Vacuum-assisted HPDC has been the main application

direction. However, the effect of parameters on microstructure and thermal conductivity is complex, and research on fully elucidating the effect mechanism of processing on solute contents, eutectics, and porosity is still inadequate. Therefore, aiming at different die-cast alloys, how to adjust and optimize the processing parameters reasonably remains a critical factor and challenge to obtain die castings with excellent properties. With the development of commercial software, the optimization of the processing parameters of die-cast aluminum alloys with high thermal conductivity with the help of advanced software is a feasible method.

5. Heat Treatment for Die-Cast Aluminum Alloys

In die-cast aluminum alloys, the common heat treatment methods consist of solution treatment and aging treatment [137–139]. The solution treatment involves the transfer of atoms in precipitates into solid solutions as solutes with variations in solubility at different temperatures. Then, the alloy is quenched to maintain the supersaturated solid solutions at room temperature. Next, aging treatment should be carried out to precipitate these solutes at a lower temperature compared to the solution treatment. In general, equipped with different aging treatments, there are four heat treatment methods [140]: solution treatment and natural aging (T4), solution treatment and artificial under-aging (T5), solution treatment and artificial peak aging (T6), and solution treatment and artificial over-aging (T7). Although heat treatment is not expected to be widely used in large-size thin-wall die castings because of the danger of bending and surface blistering [141], we also give a brief review on the effect of heat treatment on the thermal conductivity of die-cast aluminum alloys. The beneficial effects of heat treatment on the thermal conductivity of die-cast Al alloys can be mainly divided into the following four parts from several gravity-cast alloys:

- (1) Decreasing the number of defects like dislocations and point defects at elevated temperatures [142];
- (2) Promoting the spheroidization of eutectic Si at elevated temperatures [143];
- (3) Promoting precipitations like Mg_2Si from the solid solutions during the aging process [144];
- (4) Controlling the interfacial structure to be semi-coherent or incoherent during the aging process [145].

In die-cast Al alloys, Lumley et al. [61,146] conducted excellent work on the heat treatment of Al–Si die castings. After T4, T6, and T7 processes, the thermal conductivity of the A380 die casting increased from $\sim 110 \text{ W m}^{-1} \text{ K}^{-1}$ (as-cast state) to $\sim 120 \text{ W m}^{-1} \text{ K}^{-1}$ (T4), $\sim 129 \text{ W m}^{-1} \text{ K}^{-1}$ (T6), and $\sim 135 \text{ W m}^{-1} \text{ K}^{-1}$ (T7) because of the spheroidization of eutectic Si and a large number of fine dispersions of precipitate Al_2Cu phases. In addition, more Al–Si die castings were treated under the T7 process for one hour and showed improvements in both thermal conductivity and mechanical properties. Alloy 5 (Al–7.2Si–1.8Cu–0.24Fe–0.46Mn–0.22Mg–0.43Zn–0.1Ti) with lower contents of alloying elements, especially Si, had a lower increase in thermal conductivity. J.K. Chen et al. [123] also confirmed the spheroidization behavior of eutectic Si in the Al–Si die casting and with an increase in the time of T6 heat treatment, thermal conductivity increased. In rheological Al–Si die castings, a T6 peak aging heat treatment could also increase the thermal conductivity from $153 \text{ W m}^{-1} \text{ K}^{-1}$ to $182 \text{ W m}^{-1} \text{ K}^{-1}$ [75]. The increases in thermal conductivity by solution and aging heat treatment have been listed in Table 4. It is shown that the T4 process with natural aging results in a low improvement in thermal conductivity and the T7 process has a higher increase. If the alloy contains more alloying elements, especially Cu, Mg, and Zn, which have a large variation in solubility under different temperatures, the enhancement of thermal conductivity can be more obvious.

Table 4. Thermal conductivity of die-cast aluminum alloys after heat treatment.

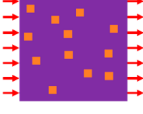
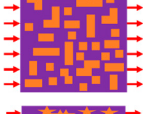
Alloy	Heat Treatment	Thermal Conductivity (W m ⁻¹ K ⁻¹)	Improvement Ratio (%)	Ref.
A380	T4	120	9.1	[146]
A380	T6	129	17.3	[146]
A380	T7	135	22.7	[146]
Al-10.5Si-1.75Cu-0.71Fe-0.16Mn-0.23Mg-0.76Zn	T7	155	61.6	[61]
Al-10.6Si-2.41Cu-0.85Fe-0.2Mn-0.22Mg-0.75Zn	T7	150	59.8	[61]
Al-10.07Si-2.16Cu-0.25Fe-0.49Mn-0.1Mg	T7	125	16.2	[61]
Al-10.4Si-2.25Cu-0.25Fe-0.47Mn-0.22Mg	T7	117	16.9	[61]
Al-7.2Si-1.8Cu-0.24Fe-0.46Mn-0.22Mg-0.43Zn-0.1Ti	T7	121	12.6	[61]
Al-10Si-0.6Cu-0.9Fe-0.7Zn	T4	147	16.2	[123]
Al-10Si-0.6Cu-0.9Fe-0.7Zn	T6 (1 h)	149	17.1	[123]
Al-10Si-0.6Cu-0.9Fe-0.7Zn	T6 (4 h)	152	19.6	[123]

Recently, direct aging treatment without solution treatment was also used to increase the thermal conductivity and mechanical properties of Al alloys. Camille et al. [147] tried to use direct aging to optimize the electrical conductivity (17 MS m⁻¹ → 26.5 MS m⁻¹) and yield strength (134~137 MPa → 334~337 MPa) successfully by mainly precipitating Al₃Zr fine precipitates in Al-Fe-Zr alloy. Another work also used the direct aging process at 180 °C in Al-Ni-Mg-Si conductor cast alloys. After the aging treatment, the microhardness and electrical conductivity both increased mainly because β' and β'' nanoparticles precipitated from the substrate [148]. This kind of method is suitable for aluminum die castings because of the supersaturated solid solutions. Additionally, the aging treatment can also omit the solution treatment with a very high temperature to avoid the die castings being discarded. However, studies regarding this method in die casting to optimize thermal conductivity are still limited and worth deeply investigating.

6. Models of Thermal Conductivity for Die-Cast Aluminum Alloys

To date, plenty of theoretical models have been applied to aluminum alloys. Matthiessen's rule mentioned in Section 3 was widely used in predicting the thermal conductivity of aluminum alloys and studying the effect of alloying elements on electrical conductivity and thermal conductivity in combination with the Wiedemann–Franz law [58,60]. However, this model only considers the effect of alloying element contents on thermal conductivity. Further, the calculation of Matthiessen's rule depends on ρ_s^i and ρ_p^i . The reported values of these two parameters do not cover all elements such as rare elements. Thus, it is important to expand the database of ρ_s^i and ρ_p^i to apply this model further. In addition, in real alloys, the distribution of different components and their shape also affect thermal conductivity and should be considered. Therefore, considering aluminum alloys as composites, many models on the effective thermal conductivity of two-component composites are proposed. The formulas are listed in Table 5. The series model and parallel model were built to address the situation where phases are perpendicular and parallel to the heat dissipation direction [149]. In general, the distribution of phases in alloys is not parallel or perpendicular; the series model and parallel model are the lower and upper boundaries of the real thermal conductivity. Furthermore, combining series and parallel models, a model suitable for lamellar eutectics was calculated [150]. For more situations, aimed at dispersive phases, a Maxwell–Eucken model was proposed [149,151]. The model supposes that the dispersive phase is distributed in the continuous phase and the distance of the dispersive phase should be long enough that they cannot interact with each other. Two-form equations are listed in Table 5 according to relative values of the thermal conductivity of dispersive and continuous phases. Furthermore, considering the effect of morphology of dispersive phases, a modified Maxwell–Eucken model is established in Table 5 [151,152]. For cases involving interactions between different dispersive phases, an effective medium model was deduced [149]. Like the modified Maxwell–Eucken model, a general effective medium model was further obtained considering geometry and distribution parameters [151,153] and is listed in Table 5.

Table 5. Thermal conductivity models of two-component composites for aluminum alloys.

Model	Phase Arrangement	Formula	Refs.
Series model		$\lambda_s = \left(\frac{V_1}{\lambda_1} + \frac{V_2}{\lambda_2} \right)^{-1}$	[149]
Parallel model		$\lambda_p = V_1 \lambda_1 + V_2 \lambda_2$	[149]
Eutectic model (lamellae)		$\lambda = \frac{1}{4} \left[\lambda_p + \sqrt{\lambda_p^2 + 8 \lambda_p \lambda_s} \right]$	[150]
Maxwell–Eucken model 1 (λ_1 : continuous phase, λ_2 : dispersive phase, $\lambda_1 > \lambda_2$)		$\lambda = \lambda_1 \left[\frac{\lambda_2 + 2\lambda_1 - 2V_2(\lambda_1 - \lambda_2)}{\lambda_2 + 2\lambda_1 + V_2(\lambda_1 - \lambda_2)} \right]$	[149,151]
Maxwell–Eucken model 2 (λ_1 : dispersive phase, λ_2 : continuous phase, $\lambda_1 > \lambda_2$)		$\lambda = \lambda_2 \left[\frac{\lambda_1 + 2\lambda_2 - 2V_1(\lambda_2 - \lambda_1)}{\lambda_1 + 2\lambda_2 + V_1(\lambda_2 - \lambda_1)} \right]$	[149,151]
Modified Maxwell–Eucken model		$\lambda = \lambda_1 \left[\frac{\lambda_2 + (n-1)\lambda_1 - (n-1)V_2(\lambda_1 - \lambda_2)}{\lambda_2 + (n-1)\lambda_1 + V_2(\lambda_1 - \lambda_2)} \right]$	[151,152]
Effective medium model		$V_1 \frac{\lambda_1 - \lambda}{\lambda_1 + 2\lambda} + V_2 \frac{\lambda_2 - \lambda}{\lambda_2 + 2\lambda} = 0$	[149]
General effective medium model		$V_1 \frac{\lambda_1^{1/t} - \lambda^{1/t}}{\lambda_1^{1/t} + A\lambda^{1/t}} + V_2 \frac{\lambda_2^{1/t} - \lambda^{1/t}}{\lambda_2^{1/t} + A\lambda^{1/t}} = 0$	[151,153]

In die-cast Al alloys, there are few related studies on the theoretical calculation of thermal conductivity. Thermal conductivity considering porosity was calculated by the Maxwell–Eucken model [123]. They set the thermal conductivity of pores to zero and successfully calculated the total thermal conductivity of die casting. Lumley et al. [61] used Matthiessen’s rule and the Wiedemann–Franz law to calculate the as-cast and heat-treated Al–Si high-pressure die castings. In the work, the calculation was similar to experiment results. However, the solute concentrations of alloying elements were supposed and estimated in all Al grains, and the values were assumed to be the same for each element. For die-cast alloys, the microstructure is complex, including ESCs and α -Al in the die cavity for primary phases, and the Al solid solutions are supersaturated [154]. This indicates that the solute concentration is difficult to directly estimate from the phase diagram. Therefore, using Matthiessen’s rule to calculate the thermal conductivity of die castings is simplistic and cannot fully reflect the relationship between different parts of the microstructure. Accordingly, in order to understand the relationship between microstructure and thermal conductivity accurately, a new model applied for die-cast alloys should be proposed in the future.

7. Conclusions and Perspectives

This review summarized the thermal conductivity of high-pressure die-cast aluminum alloys from fundamental theory, alloy development, casting processing parameters, heat

treatment strategies, and numerical models. Several conclusions and perspectives are written as follows:

- (1) In aluminum alloys, the thermal conductivity can be divided into electrical thermal conductivity and phonon thermal conductivity. The former is dominant in aluminum alloys. As a whole, the fundamental theory of the electrical heat conduction in aluminum alloys is abundant. For the phonon thermal conductivity, the relationship between the phonon thermal conductivity and temperature is clear. However, deep studies about the relationship between the phonon thermal conductivity and alloy compositions in aluminum alloys are lacking and can be performed further.
- (2) For alloy development, the Al–Si system is still the main system of die-cast alloys used for heat dissipation components. Reducing the major elements and adding trace elements to optimize the microstructure through decreasing solute concentrations in the substrate and modifying eutectic particles are the main methods used to improve thermal conductivity of alloys. In order to obtain higher thermal conductivity, a series of die-cast Al alloys only containing Fe or Ni are developed. However, more studies on the relationship between thermal conductivity and microstructure under the die-cast condition are needed. In addition, the mechanical properties of the alloys need to be improved for applications while ensuring high thermal conductivity and castability.
- (3) The thermal conductivity of die-cast aluminum alloys is affected by microstructure and porosity under different processing parameters. Moreover, the rheological die-casting process can improve the thermal conductivity and mechanical properties synergistically. However, the definite influence relationships between processing and thermal conductivity are still insufficient and needed. Strategies to optimize the die-casting processing parameters for die-cast alloys with highly comprehensive properties are also of great interest for future studies. The optimization of processing parameters of die-cast aluminum alloys with high thermal conductivity with the help of advanced software is a feasible method.
- (4) Solution and aging heat treatment processes can improve the thermal conductivity of die-cast aluminum alloys mainly through the precipitation from solid solutions and the spheroidization of eutectics. The T7 process has a significant increase in thermal conductivity of die-cast alloys. To adjust the requirement of the trend of large-size die castings, the direct aging process after casting, which can be applied to improve the comprehensive properties of die-cast alloys, is worthy of further studies.
- (5) Many theoretical models of composites have been proposed to calculate the thermal conductivity of aluminum alloys, and some of them have been used in die-cast alloys. However, a single model cannot describe the complex microstructure formed in multiple steps during the die-casting process. Therefore, to comprehensively understand the relationship between the microstructure and thermal conductivity in die-cast alloys, a new thermal conductivity calculation model for die-cast alloys needs to be built.

In summary, numerous excellent works have been performed to develop high-thermal-conductivity die-cast aluminum alloys, and many of them have been used successfully in industry. However, in each part of this review, the number of studies on the thermal conductivity of gravity-cast alloys is larger than that of die-cast alloys. Therefore, scientific studies on die-cast aluminum alloys with high thermal conductivity should be enhanced in the future and are expected to guide the development of new aluminum alloys for industrial applications.

Author Contributions: Y.L.: Methodology, Investigation, Formal analysis, Writing—original draft, Writing—review and editing. S.X.: Funding acquisition, Resources, Validation, Writing—review and editing, Supervision. All authors have read and agreed to the published version of the manuscript.

Funding: We acknowledge funding support from the National Natural Science Foundation of China (Grant No. 52175335, S.X.).

Data Availability Statement: Not applicable.

Conflicts of Interest: The authors declare no conflicts of interest.

References

1. Sun, Y. The Use of Aluminum Alloys in Structures: Review and Outlook. *Structures* **2023**, *57*, 105290. [CrossRef]
2. You, X.; Xing, Z.; Jiang, S.; Zhu, Y.; Lin, Y.; Qiu, H.; Nie, R.; Yang, J.; Hui, D.; Chen, W.; et al. A Review of Research on Aluminum Alloy Materials in Structural Engineering. *Dev. Built Environ.* **2024**, *17*, 100319. [CrossRef]
3. Mondolfo, L.F. *Aluminium Alloys: Structure and Properties*, 2nd ed.; Butterworths: London, UK, 1979; ISBN 978-0-408-70932-3.
4. Aluminium Applications—Construction. Available online: <https://aluminiumleader.com/application/construction/> (accessed on 7 January 2024).
5. Yaroshevsky, A.A. Abundances of Chemical Elements in the Earth's Crust. *Geochem. Int.* **2006**, *44*, 48–55. [CrossRef]
6. Bhagtani, P.; Bichler, L.; Bardelcik, A.; Elsayed, A. Modeling Thermal Conductivity of Al-Ni, Al-Fe, and Al-Co Spark Plasma Sintered Alloys. *J. Mater. Eng. Perform.* **2023**, *32*, 6821–6832. [CrossRef]
7. Hirsch, J. Recent Development in Aluminium for Automotive Applications. *Trans. Nonferrous Met. Soc. China* **2014**, *24*, 1995–2002. [CrossRef]
8. Markaustin Aluminium—The Green Metal. Available online: <https://www.hazlemerecommercial.co.uk/blog/aluminium-the-green-metal/2012/04/> (accessed on 7 January 2024).
9. Mills, K.C. *Recommended Values of Thermophysical Properties for Selected Commercial Alloys*; Woodhead: Cambridge, UK, 2002; ISBN 978-1-85573-569-9.
10. Klemens, P.G. *Thermal Conductivity of Pure Metals and Alloys*; Springer: Berlin/Heidelberg, Germany, 1991.
11. Haynes, W.M. *CRC Handbook of Chemistry and Physics*, 96th ed.; CRC Press: Boca Raton, FL, USA, 2015.
12. Jiao, X.Y.; Wang, P.Y.; Liu, Y.X.; Wang, J.; Liu, W.N.; Wan, A.X.; Shi, L.J.; Wang, C.G.; Xiong, S.M. Fracture Behavior of a High Pressure Die Casting AlSi10MnMg Alloy with Varied Porosity Levels. *J. Mater. Res. Technol.* **2023**, *25*, 1129–1140. [CrossRef]
13. Chen, Z.W. Formation and Progression of Die Soldering during High Pressure Die Casting. *Mater. Sci. Eng. A* **2005**, *397*, 356–369. [CrossRef]
14. Hu, L.; Chen, S.; Miao, Y.; Meng, Q. Die-Casting Effect on Surface Characteristics of Thin-Walled AZ91D Magnesium Components. *Appl. Surf. Sci.* **2012**, *261*, 851–856. [CrossRef]
15. Kang, C.G.; Lee, S.M.; Kim, B.-M. A Study of Die Design of Semi-Solid Die Casting According to Gate Shape and Solid Fraction. *J. Mater. Process. Technol.* **2008**, *204*, 8–21. [CrossRef]
16. Li, X. Study on Externally Solidified Crystals and Their Relationship with the Defects and Mechanical Properties of High Pressure Die Cast Magnesium Alloys. Ph.D. Thesis, Tsinghua University, Beijing, China, 2017.
17. Liu, W.; Zhang, W.; Wang, P.; Liu, Y.; Jiao, X.; Wan, A.; Wang, C.; Tong, G.; Xiong, S. Effect of Slow Shot Speed on Externally Solidified Crystal, Porosity and Tensile Property in a Newly Developed High-Pressure Die-Cast Al-Si Alloy. *China Foundry* **2023**, *21*, 11–19. [CrossRef]
18. Jiao, X.Y.; Wang, J.; Liu, C.; Guo, Z.; Wang, J.; Wang, Z.; Gao, J.; Xiong, S.M. Influence of Slow-Shot Speed on PSPs and Porosity of AlSi17Cu2.5 Alloy during High Pressure Die Casting. *J. Mater. Process. Technol.* **2019**, *268*, 63–69. [CrossRef]
19. Jiao, X.Y.; Liu, C.F.; Guo, Z.P.; Nishat, H.; Tong, G.D.; Ma, S.L.; Bi, Y.; Zhang, Y.F.; Wiesner, S.; Xiong, S.M. On the Characterization of Primary Iron-Rich Phase in a High-Pressure Die-Cast Hypoeutectic Al-Si Alloy. *J. Alloys Compd.* **2021**, *862*, 158580. [CrossRef]
20. Li, X.-B.; Xiong, S.-M.; Guo, Z.-P. Characterization of the Grain Structures in Vacuum-Assist High-Pressure Die Casting AM60B Alloy. *Acta Metall. Sin. Engl. Lett.* **2016**, *29*, 619–628. [CrossRef]
21. Guo, Z.-P.; Xiong, S.-M.; Liu, B.-C.; Li, M.; Allison, J. Effect of Process Parameters, Casting Thickness, and Alloys on the Interfacial Heat-Transfer Coefficient in the High-Pressure Die-Casting Process. *Metall. Mater. Trans. A* **2008**, *39*, 2896–2905. [CrossRef]
22. Luo, A.A.; Sachdev, A.K.; Apelian, D. Alloy Development and Process Innovations for Light Metals Casting. *J. Mater. Process. Technol.* **2022**, *306*, 117606. [CrossRef]
23. Li, X.; Xiong, S.M.; Guo, Z. Improved Mechanical Properties in Vacuum-Assist High-Pressure Die Casting of AZ91D Alloy. *J. Mater. Process. Technol.* **2016**, *231*, 1–7. [CrossRef]
24. Gan, J.; Huang, Y.; Wen, C.; Du, J. Effect of Sr Modification on Microstructure and Thermal Conductivity of Hypoeutectic Al–Si Alloys. *Trans. Nonferrous Met. Soc. China* **2020**, *30*, 2879–2890. [CrossRef]
25. Families of Alloys—RHEINFELDEN ALLOYS. Available online: <https://rheinfelden-alloys.eu/en/alloys/> (accessed on 7 January 2024).
26. Wang, Y.; Kang, H.; Guo, Y.; Chen, H.; Hu, M.; Ji, Z. Design and Preparation of Aluminum Alloy with High Thermal Conductivity Based on CALPHAD and First-Principles Calculation. *China Foundry* **2022**, *19*, 225–237. [CrossRef]
27. Li, T.; Song, J.; Zhang, A.; You, G.; Yang, Y.; Jiang, B.; Qin, X.; Xu, C.; Pan, F. Progress and Prospects in Mg-Alloy Super-Sized High Pressure Die Casting for Automotive Structural Components. *J. Magnes. Alloys* **2023**, *11*, 4166–4180. [CrossRef]
28. Li, Y.; Chen, J.; Agrawal, P.; Feng, Z. Microstructure and Mechanical Properties of Ultrasonic Spot Welding of AA7075-T6 and A380 Casting Aluminum Alloy. *J. Manuf. Process.* **2024**, *110*, 126–133. [CrossRef]
29. Liu, W.; Zhao, C.; Kishita, Y.; Wan, A.; Peng, T.; Umeda, Y. Scenario Analysis on Carbon Peaking Pathways for China's Aluminum Casting Industry. *J. Clean. Prod.* **2023**, *422*, 138571. [CrossRef]

30. Technology—Mega-Casting—AMS January–March 2022. Available online: https://automotivemanufacturingsolutions.h5mag.com/ams_january-march_2022/technology_mega-casting (accessed on 9 January 2024).
31. Toyota Showcases Its Own Giga Casting in a Bid to Lower EV Costs. Available online: <https://insideevs.com/news/671943/toyota-giga-casting/> (accessed on 9 January 2024).
32. VW’s Project Trinity to Use Giga-Casting & Automation to Compete with Tesla. Available online: <https://insideevs.com/news/577128/volkswagen-compete-tesla-gigapress-robots/> (accessed on 9 January 2024).
33. Sharma, A.; Morisada, Y.; Fujii, H. Influence of Aluminium-Rich Intermetallics on Microstructure Evolution and Mechanical Properties of Friction Stir Alloyed Al Fe Alloy System. *J. Manuf. Process.* **2021**, *68*, 668–682. [CrossRef]
34. Li, Y.; Hu, A.; Fu, Y.; Liu, S.; Shen, W.; Hu, H.; Nie, X. Al Alloys and Casting Processes for Induction Motor Applications in Battery-Powered Electric Vehicles: A Review. *Metals* **2022**, *12*, 216. [CrossRef]
35. Jiao, X.Y.; Wang, J.; Liu, C.F.; Guo, Z.P.; Tong, G.D.; Ma, S.L.; Bi, Y.; Zhang, Y.F.; Xiong, S.M. Characterization of High-Pressure Die-Cast Hypereutectic Al-Si Alloys Based on Microstructural Distribution and Fracture Morphology. *J. Mater. Sci. Technol.* **2019**, *35*, 1099–1107. [CrossRef]
36. Qi, M.; Kang, Y.; Xu, Y.; Wulabieke, Z.; Li, J. A Novel Rheological High Pressure Die-Casting Process for Preparing Large Thin-Walled Al-Si-Fe-Mg-Sr Alloy with High Heat Conductivity, High Plasticity and Medium Strength. *Mater. Sci. Eng. A* **2020**, *776*, 139040. [CrossRef]
37. ADC12 Aluminum A383 | Equivalent Materials & Metal Specifications. Available online: <https://redstonemanufacturing.com/adc12-aluminum/> (accessed on 9 January 2024).
38. Aluminium Alloy A380 properties | OEFORM. Available online: <https://oeform.com/die-cast-aluminium-alloy-a380-properties/> (accessed on 9 January 2024).
39. A360 Aluminum Properties | Die Cast Materials. Available online: <https://www.dynacast.com/en/knowledge-center/material-information/aluminum-die-casting-metals/a360> (accessed on 9 January 2024).
40. 384.0 (384.0-F, SC114A, A03840) Cast Aluminum: MakeItFrom.Com. Available online: <https://www.makeitfrom.com/material-properties/384.0-384.0-F-SC114A-A03840-Cast-Aluminum> (accessed on 9 January 2024).
41. Aluminum Alloy 413 Properties | Aluminum Die Casting. Available online: <https://www.dynacast.com/en/knowledge-center/material-information/aluminum-die-casting-metals/413> (accessed on 9 January 2024).
42. Etxandi-Santolaya, M.; Canals Casals, L.; Corchero, C. Estimation of Electric Vehicle Battery Capacity Requirements Based on Synthetic Cycles. *Transp. Res. Part Transp. Environ.* **2023**, *114*, 103545. [CrossRef]
43. Ma, S.; Jiang, M.; Tao, P.; Song, C.; Wu, J.; Wang, J.; Deng, T.; Shang, W. Temperature Effect and Thermal Impact in Lithium-Ion Batteries: A Review. *Prog. Nat. Sci. Mater. Int.* **2018**, *28*, 653–666. [CrossRef]
44. Hardesty, L. 5G Base Stations Use a Lot More Energy than 4G Base Stations: MTN | Fierce Wireless. Available online: <https://www.fiercewireless.com/tech/5g-base-stations-use-a-lot-more-energy-than-4g-base-stations-says-mtn> (accessed on 10 January 2024).
45. Solkin, M. Electromagnetic Interference Hazards in Flight and the 5G Mobile Phone: Review of Critical Issues in Aviation Security. *Transp. Res. Procedia* **2021**, *59*, 310–318. [CrossRef]
46. Chou, D. Infrastructure. In *Practical Guide to Clinical Computing Systems*; Elsevier: Amsterdam, The Netherlands, 2015; pp. 39–70. ISBN 978-0-12-420217-7.
47. Yuan, Z.; Guo, Z.; Xiong, S. Microstructure Evolution of Modified Die-Cast AlSi10MnMg Alloy during Solution Treatment and Its Effect on Mechanical Properties. *Trans. Nonferrous Met. Soc. China* **2019**, *29*, 919–930. [CrossRef]
48. Yuan, Z.; Guo, Z.; Xiong, S.M. Effect of As-Cast Microstructure Heterogeneity on Aging Behavior of a High-Pressure Die-Cast A380 Alloy. *Mater. Charact.* **2018**, *135*, 278–286. [CrossRef]
49. Li, S.; Yang, X.; Hou, J.; Du, W. A Review on Thermal Conductivity of Magnesium and Its Alloys. *J. Magnes. Alloys* **2020**, *8*, 78–90. [CrossRef]
50. Tritt, T.M. *Thermal Conductivity: Theory, Properties, and Applications*; Physics of solids and liquids; Springer: New York, NY, USA, 2004; ISBN 978-0-306-48327-1.
51. Wen, C.; Gan, J.; Li, C.; Huang, Y.; Du, J. Comparative Study on Relationship between Modification of Si Phase and Thermal Conductivity of Al-7Si Alloy Modified by Sr/RE/B/Sb Elements. *Int. J. Met.* **2021**, *15*, 194–205. [CrossRef]
52. Huang, Y.Y.; Hu, Z.L.; Wang, J.J. Research Progress on the Aluminum Alloy with High Thermal Conductivity. *Appl. Mech. Mater.* **2014**, *574*, 396–400. [CrossRef]
53. Stojanovic, N.; Maithripala, D.H.S.; Berg, J.M.; Holtz, M. Thermal Conductivity in Metallic Nanostructures at High Temperature: Electrons, Phonons, and the Wiedemann-Franz Law. *Phys. Rev. B* **2010**, *82*, 075418. [CrossRef]
54. Han, S.; Dai, S.; Ma, J.; Ren, Q.; Hu, C.; Gao, Z.; Duc Le, M.; Sheptyakov, D.; Miao, P.; Torii, S.; et al. Strong Phonon Softening and Avoided Crossing in Aliovalence-Doped Heavy-Band Thermoelectrics. *Nat. Phys.* **2023**, *19*, 1649–1657. [CrossRef]
55. Luckyanova, M.N.; Mendoza, J.; Lu, H.; Song, B.; Huang, S.; Zhou, J.; Li, M.; Dong, Y.; Zhou, H.; Garlow, J.; et al. Phonon Localization in Heat Conduction. *Sci. Adv.* **2018**, *4*, eaat9460. [CrossRef] [PubMed]
56. Cook, J.G.; Moore, J.P.; Matsumura, T.; Van Der Meer, M.P. The Thermal and Electrical Conductivity of Aluminum. In *Thermal Conductivity 14*; Klemens, P.G., Chu, T.K., Eds.; Springer: Boston, MA, USA, 1976; pp. 65–71. ISBN 978-1-4899-3753-7.
57. Klemens, P.G.; Williams, R.K. Thermal Conductivity of Metals and Alloys. *Int. Met. Rev.* **1986**, *31*, 197–215. [CrossRef]
58. Zhang, A.; Li, Y. Effect of Alloying Elements on Thermal Conductivity of Aluminum. *J. Mater. Res.* **2023**, *38*, 2049–2058. [CrossRef]
59. Lumley, R.N. *Fundamentals of Aluminium Metallurgy*; Woodhead Publishing: Cambridge, UK, 2018; ISBN 978-0-08-102063-0.

60. Olafsson, P.; Sandstrom, R.; Karlsson, Å. Comparison of Experimental, Calculated and Observed Values for Electrical and Thermal Conductivity of Aluminium Alloys. *J. Mater. Sci.* **1997**, *32*, 4383–4390. [[CrossRef](#)]
61. Lumley, R.N.; Deeva, N.; Larsen, R.; Gembarovic, J.; Freeman, J. The Role of Alloy Composition and T7 Heat Treatment in Enhancing Thermal Conductivity of Aluminum High Pressure Diecastings. *Metall. Mater. Trans. A* **2013**, *44*, 1074–1086. [[CrossRef](#)]
62. Karabay, S. Modification of AA-6201 Alloy for Manufacturing of High Conductivity and Extra High Conductivity Wires with Property of High Tensile Stress after Artificial Aging Heat Treatment for All-Aluminium Alloy Conductors. *Mater. Des.* **2006**, *27*, 821–832. [[CrossRef](#)]
63. Jing, L.; Cheng, W.; Gan, J. Influencing Mechanisms of Alloying Elements on the Electrical Conductivity of Pure Aluminum. *Mater. Rep.* **2021**, *35*, 24101–24106. [[CrossRef](#)]
64. Chen, J.K.; Hung, H.Y.; Wang, C.F.; Tang, N.K. Thermal and Electrical Conductivity in Al-Si/Cu/Fe/Mg Binary and Ternary Al Alloys. *J. Mater. Sci.* **2015**, *50*, 5630–5639. [[CrossRef](#)]
65. Ashiri, R.; Karimzadeh, F.; Niroumand, B. On Effect of Squeezing Pressure on Microstructural Characteristics, Heat Treatment Response and Electrical Conductivity of an Al-Si-Mg-Ni-Cu Alloy. *Mater. Sci. Technol.* **2014**, *30*, 1162–1169. [[CrossRef](#)]
66. Jiao, X.Y.; Liu, Y.X.; Wang, J.; Liu, W.N.; Wan, A.X.; Wiesner, S.; Xiong, S.M. The Microstructure Characteristics and Fracture Behavior of the Polyhedral Primary Iron-Rich Phase and Plate-Shaped Eutectic Iron-Rich Phase in a High-Pressure Die-Cast AlSi10MnMg Alloy. *J. Mater. Sci. Technol.* **2023**, *140*, 201–209. [[CrossRef](#)]
67. Jiao, X.Y.; Zhang, W.; Liu, Y.X.; Wang, J.; Liu, W.N.; Wan, A.X.; Hu, Y.Y.; Tong, G.D.; Xiong, S.M. The Characterization of Porosity and Its Relationship with Externally Solidified Crystal in a High-Pressure Die-Cast AlSi10MnMg Alloy via a Laboratory CT Technique. *Mater. Lett.* **2023**, *335*, 133807. [[CrossRef](#)]
68. Cingi, C.; Rauta, V.; Suikkanen, E.; Orkas, J. Effect of Heat Treatment on Thermal Conductivity of Aluminum Die Casting Alloys. *Adv. Mater. Res.* **2012**, *538–541*, 2047–2052. [[CrossRef](#)]
69. Jiao, X.Y.; Zhang, Y.F.; Wang, J.; Nishat, H.; Liu, Y.X.; Liu, W.N.; Chen, H.X.; Xiong, S.M. Characterization of Externally Solidified Crystals in a High-Pressure Die-Cast AlSi10MnMg Alloy and Their Effect on Porosities and Mechanical Properties. *J. Mater. Process. Technol.* **2021**, *298*, 117299. [[CrossRef](#)]
70. Lin, S.; Dang, J.; Wang, Z.; Sun, Y.; Xiang, Y. Enhanced Strength and Toughness in Al-Mg-Si Alloys with Addition of Cr, Mn, and Cu Elements. *J. Mater. Eng. Perform.* **2023**, *32*, 1039–1050. [[CrossRef](#)]
71. Cui, X. Research on the Influence Mechanisms of Melt Complex Boron Treatment and Second Phases Morphological Evolution on Electrical Conductivity of Aluminum Alloys. Ph.D. Thesis, Shandong University, Jinan, China, 2016.
72. Qin, Y.; Yan, Z.; Wu, Q.; Jiang, A.; Li, Y.; Ma, S.; Lü, S.; Li, J. Development of a Novel High Strength Al-Si-Cu-Ni Alloy by Combining Micro-Alloying and Squeeze Casting. *J. Alloys Compd.* **2023**, *967*, 171780. [[CrossRef](#)]
73. Zhai, W.; Sun, H.; Sun, L.; Zhao, Q.; Liu, Y.; Wang, Y.; Pu, B.; Zhang, B.; Wang, S. Influence of Cu Content on Mechanical and Tribological Properties of Al-7Si-Cu Alloy. *J. Mater. Res. Technol.* **2023**, *26*, 4848–4859. [[CrossRef](#)]
74. Qi, M.; Kang, Y.; Qiu, Q.; Tang, W.; Li, J.; Li, B. Microstructures, Mechanical Properties, and Corrosion Behavior of Novel High-Thermal-Conductivity Hypoeutectic Al-Si Alloys Prepared by Rheological High Pressure Die-Casting and High Pressure Die-Casting. *J. Alloys Compd.* **2018**, *749*, 487–502. [[CrossRef](#)]
75. Payandeh, M.; Sjölander, E.; Jarfors, A.E.W.; Wessén, M. Influence of Microstructure and Heat Treatment on Thermal Conductivity of Rheocast and Liquid Die Cast Al-6Si-2Cu-Zn Alloy. *Int. J. Cast Met. Res.* **2016**, *29*, 202–213. [[CrossRef](#)]
76. Jang, J.-C.; Shin, K.S. Effects of Ni and Cu Addition on Tensile Properties and Thermal Conductivity of High Pressure Die-cast Al-6Si Alloys. *Korean J. Met. Mater.* **2020**, *58*, 217–226. [[CrossRef](#)]
77. Samuel, A.M.; Gauthier, J.; Samuel, F.H. Microstructural Aspects of the Dissolution and Melting of Al₂Cu Phase in Al-Si Alloys during Solution Heat Treatment. *Metall. Mater. Trans. A* **1996**, *27*, 1785–1798. [[CrossRef](#)]
78. Choi, S.W.; Cho, H.S.; Kumai, S. Effect of the Precipitation of Secondary Phases on the Thermal Diffusivity and Thermal Conductivity of Al-4.5Cu Alloy. *J. Alloys Compd.* **2016**, *688*, 897–902. [[CrossRef](#)]
79. Vandersluis, E.; Ravindran, C. Effects of Solution Heat Treatment Time on the As-Quenched Microstructure, Hardness and Electrical Conductivity of B319 Aluminum Alloy. *J. Alloys Compd.* **2020**, *838*, 155577. [[CrossRef](#)]
80. Kumar, L.; Jang, J.C.; Yu, H.; Shin, K.S. Effect of Secondary Phase on Mechanical and Thermal Conductivity of Al-Si-xFe-Mg-yCu-Mn Die Casting Alloys. *Mater. Lett.* **2022**, *314*, 131889. [[CrossRef](#)]
81. Kumar, L.; Jang, J.C.; Yu, H.; Shin, K.S. Effects of Cr and Ti Addition on Mechanical Properties and Thermal Conductivity of Al-7Si-3Mg Die-Casting Alloys. *Met. Mater. Int.* **2023**, *29*, 204–214. [[CrossRef](#)]
82. Kim, C.W.; Cho, J.I.; Choi, S.W.; Kim, Y.C. The Effect of Alloying Elements on Thermal Conductivity of Aluminum Alloys in High Pressure Die Casting. *Adv. Mater. Res.* **2013**, *813*, 175–178. [[CrossRef](#)]
83. Kim, C.-W.; Kim, Y.-C.; Kim, J.-H.; Cho, J.-I.; Oh, M.-S. Effect of Alloying Elements on the Thermal Conductivity and Casting Characteristics of Aluminum Alloys in High Pressure Die Casting. *Korean J. Met. Mater.* **2018**, *56*, 805–812. [[CrossRef](#)]
84. Cho, Y.H.; Kim, H.W.; Lee, J.M.; Kim, M.S. A New Approach to the Design of a Low Si-Added Al-Si Casting Alloy for Optimising Thermal Conductivity and Fluidity. *J. Mater. Sci.* **2015**, *50*, 7271–7281. [[CrossRef](#)]
85. Becker, H.; Bergh, T.; Vullum, P.E.; Leineweber, A.; Li, Y. β - and δ -Al-Fe-Si Intermetallic Phase, Their Intergrowth and Polytype Formation. *J. Alloys Compd.* **2019**, *780*, 917–929. [[CrossRef](#)]
86. Becker, H.; Bergh, T.; Vullum, P.E.; Leineweber, A.; Li, Y. Effect of Mn and Cooling Rates on α -, β - and δ -Al-Fe-Si Intermetallic Phase Formation in a Secondary Al-Si Alloy. *Materialia* **2019**, *5*, 100198. [[CrossRef](#)]

87. Zhao, J.; Guo, Y.; Xu, B.; Gu, C.; Wang, Y.; Tang, Q. Effect of Microstructure Evolution of Iron-Rich Intermetallic Compounds on Mechanical Property of Al–7Si–0.3Mg Casting Alloy with Low Iron Content. *Metall. Mater. Trans. B* **2022**, *53*, 548–560. [[CrossRef](#)]
88. Wang, M.; Hu, K.; Liu, G.; Liu, X. Synchronous Improvement of Electrical and Mechanical Performance of A356 Alloy Reinforced by Boron Coupling Nano-AlNp. *J. Alloys Compd.* **2020**, *814*, 152217. [[CrossRef](#)]
89. Ye, H.; Cui, X.; Cui, H.; Li, X.; Zhu, Z.; Pan, Y.; Feng, R. Study about Improving Mechanism of Electrical Conductivity of AA1070Al Treated by a Novel Composite Boron Treatment with Trace Ti. *J. Alloys Compd.* **2021**, *870*, 159416. [[CrossRef](#)]
90. Xu, X.; Feng, Y.; Yang, P.; Zhang, B.; Wang, Y.; Wang, Q.; Fan, X.; Ding, H. The Influence of Trace Elements on the Microstructures and Properties of the Aluminum Conductors. *Results Phys.* **2018**, *11*, 1058–1063. [[CrossRef](#)]
91. Cui, X.; Wu, Y.; Cui, H.; Zhang, G.; Zhou, B.; Liu, X. The Improvement of Boron Treatment Efficiency and Electrical Conductivity of AA1070Al Achieved by Trace Ti Assistant. *J. Alloys Compd.* **2018**, *735*, 62–67. [[CrossRef](#)]
92. Khaliq, A.; Rhamdhani, M.A.; Brooks, G.A.; Grandfield, J.F. Removal of Vanadium from Molten Aluminum—Part I. Analysis of VB₂ Formation. *Metall. Mater. Trans. B* **2014**, *45*, 752–768. [[CrossRef](#)]
93. Khaliq, A.; Rhamdhani, M.A.; Brooks, G.A.; Grandfield, J.F. Removal of Vanadium from Molten Aluminum—Part II. Kinetic Analysis and Mechanism of VB₂ Formation. *Metall. Mater. Trans. B* **2014**, *45*, 769–783. [[CrossRef](#)]
94. Khaliq, A.; Akbar Rhamdhani, M.; Brooks, G.A.; Grandfield, J. Removal of Vanadium from Molten Aluminum—Part III. Analysis of Industrial Boron Treatment Practice. *Metall. Mater. Trans. B* **2014**, *45*, 784–794. [[CrossRef](#)]
95. Yang, Z.; He, X.; Li, B.; Atrens, A.; Yang, X.; Cheng, H. Influence of Si, Cu, B, and Trace Alloying Elements on the Conductivity of the Al–Si–Cu Alloy. *Materials* **2022**, *15*, 426. [[CrossRef](#)] [[PubMed](#)]
96. Rauta, V.; Cingi, C.; Orkas, J. Effect of Annealing and Metallurgical Treatments on Thermal Conductivity of Aluminium Alloys. *Int. J. Met.* **2016**, *10*, 157–171. [[CrossRef](#)]
97. Timpel, M.; Wanderka, N.; Schlesiger, R.; Yamamoto, T.; Lazarev, N.; Isheim, D.; Schmitz, G.; Matsumura, S.; Banhart, J. The Role of Strontium in Modifying Aluminium–Silicon Alloys. *Acta Mater.* **2012**, *60*, 3920–3928. [[CrossRef](#)]
98. Moniri, S.; Shahani, A.J. Chemical Modification of Degenerate Eutectics: A Review of Recent Advances and Current Issues. *J. Mater. Res.* **2019**, *34*, 20–34. [[CrossRef](#)]
99. Lu, S.-Z.; Hellawell, A. The Mechanism of Silicon Modification in Aluminum–Silicon Alloys: Impurity Induced Twinning. *Metall. Trans. A* **1987**, *18*, 1721–1733. [[CrossRef](#)]
100. Hamilton, D.R.; Seidensticker, R.G. Propagation Mechanism of Germanium Dendrites. *J. Appl. Phys.* **1960**, *31*, 1165–1168. [[CrossRef](#)]
101. Nagaumi, H.; Wu, Y.F.; Zhu, G.L.; Xu, Y. *A Novel High Thermal Conductivity Al–Si Casting Alloy and Application*; Canadian Institute of Mining, Metallurgy and Petroleum: Montreal, QC, Canada, 2015.
102. Liu, W.; Li, Y.; Song, Z.; Luo, X.; Yang, H.; Bi, G. Effect of Trace Sr+Ce Compound Modification on Microstructure, Thermal Conductivity and Mechanical Properties of AlSi10MnMg Alloy. *Chin. J. Nonferrous Met.* **2022**, *32*, 332–342. [[CrossRef](#)]
103. Liu, W.; Li, Y.; Song, Z.; Bi, G.; Yang, H.; Cao, Y. Effect of Sr+Er Composite Modification on Microstructure, Thermal Conductivity and Mechanical Properties of AlSi10MnMg Alloy. *Mater. Rep.* **2023**, *37*, 131–137.
104. Zhang, Y.; Wei, F.; Mao, J.; Niu, G. The Difference of La and Ce as Additives of Electrical Conductivity Aluminum Alloys. *Mater. Charact.* **2019**, *158*, 109963. [[CrossRef](#)]
105. Choi, S.W.; Kim, Y.M.; Lee, K.M.; Cho, H.S.; Hong, S.K.; Kim, Y.C.; Kang, C.S.; Kumai, S. The Effects of Cooling Rate and Heat Treatment on Mechanical and Thermal Characteristics of Al–Si–Cu–Mg Foundry Alloys. *J. Alloys Compd.* **2014**, *617*, 654–659. [[CrossRef](#)]
106. Ravi, K.R.; Pillai, R.M.; Amaranathan, K.R.; Pai, B.C.; Chakraborty, M. Fluidity of Aluminum Alloys and Composites: A Review. *J. Alloys Compd.* **2008**, *456*, 201–210. [[CrossRef](#)]
107. Rohatgi, P.K.; Prabhakar, K.V. Wrought Aluminum–Nickel Alloys for High Strength–High Conductivity Applications. *Metall. Trans. A* **1974**, *6*, 1003–1008. [[CrossRef](#)]
108. Sankanit, P.; Uthaisangsuk, V.; Pandee, P. Tensile Properties of Hypoeutectic Al–Ni Alloys: Experiments and FE Simulations. *J. Alloys Compd.* **2021**, *889*, 161664. [[CrossRef](#)]
109. Palanivel, S.; Kuehmann, C.; Stucki, J.R.; Filip, E.; Edwards, P. Aluminum Alloys for Die Casting. Patent WO2020028730A1, 11 October 2019.
110. Wang, K.; Hu, S.; Zhong, Y.; Jin, S.; Zhou, Z.; Wang, Z.; Chen, J.; Wan, B.; Li, W. Effects of Trace Ytterbium Addition on Microstructure, Mechanical and Thermal Properties of Hypoeutectic Al–5Ni Alloy. *J. Rare Earths* **2022**, *40*, 1305–1315. [[CrossRef](#)]
111. Developed Alloys | Products and Services | Nikkei MC Aluminium Co., Ltd. Available online: <https://www.nmca.jp/en/product/development-alloy.html> (accessed on 7 January 2024).
112. Liu, C.; Jiao, X.; Nishat, H.; Akhtar, S.; Wiesner, S.; Guo, Z.; Xiong, S. Characteristics of Fe-Rich Intermetallics Compounds and Their Influence on the Cracking Behavior of a Newly Developed High-Pressure Die Cast Al–4Mg–2Fe Alloy. *J. Alloys Compd.* **2021**, *854*, 157121. [[CrossRef](#)]
113. Okamoto, H.; Schlesinger, M.E.; Mueller, E.M. *ASM Handbook Volume 3 Alloy Phase Diagrams*, 10th ed.; ASM International: Materials Park, OH, USA, 1990; ISBN 978-0-87170-377-4.
114. Kim, K.T.; Lim, Y.S.; Shin, J.S.; Ko, S.H.; Kim, J.M. Effects of Zn and Mg Amounts on the Properties of High Thermal Conductivity Al–Zn–Mg–Fe Alloys for Die Casting. *J. Korea Foundry Soc.* **2013**, *33*, 113–121. [[CrossRef](#)]

115. Jiang, H.; Li, S.; Zheng, Q.; Zhang, L.; He, J.; Song, Y.; Deng, C.; Zhao, J. Effect of Minor Lanthanum on the Microstructures, Tensile and Electrical Properties of Al-Fe Alloys. *Mater. Des.* **2020**, *195*, 108991. [[CrossRef](#)]
116. Luo, G.; Zhou, X.; Li, C.; Du, J.; Huang, Z. Design and Preparation of Al-Fe-Ce Ternary Aluminum Alloys with High Thermal Conductivity. *Trans. Nonferrous Met. Soc. China* **2022**, *32*, 1781–1794. [[CrossRef](#)]
117. Luo, G.; Huang, Y.; Li, C.; Huang, Z.; Du, J. Microstructures and Mechanical Properties of Al-2Fe-xCo Ternary Alloys with High Thermal Conductivity. *Materials* **2020**, *13*, 3728. [[CrossRef](#)]
118. Bian, Z.; Liu, Y.; Dai, S.; Chen, Z.; Wang, M.; Chen, D.; Wang, H. Regulating Microstructures and Mechanical Properties of Al-Fe-Ni Alloys. *Prog. Nat. Sci. Mater. Int.* **2020**, *30*, 54–62. [[CrossRef](#)]
119. Bian, Z.; Xiao, Y.; Hu, L.; Liu, Y.; Chen, Z.; Wang, M.; Chen, D.; Wang, H. Stimulated Heterogeneous Distribution of Sc Element and Its Correlated Local Hardening Effect in Al-Fe-Ni-Sc Alloy. *Mater. Sci. Eng. A* **2020**, *771*, 138650. [[CrossRef](#)]
120. Koutsoukis, T.; Makhoulouf, M.M. Alternatives to the Al-Si Eutectic System in Aluminum Casting Alloys. *Int. J. Met.* **2016**, *10*, 342–347. [[CrossRef](#)]
121. Jiang, M.; Mo, L.; Zhou, X.; Liu, X.; Zhan, M.; Du, J. Microstructure Evolution and Thermophysical Properties of Hypereutectic Al-Fe-Ni Alloys. *Int. J. Met.* **2023**, *17*, 2780–2793. [[CrossRef](#)]
122. Luo, G. Study on Microstructure Regulation and Performance of Al-Fe Based Alloys with High Thermal Conductivity. Master's Thesis, South China University of Technology, Guangzhou, China, 2021.
123. Chen, J.K.; Hung, H.Y.; Wang, C.F.; Tang, N.K. Effects of Casting and Heat Treatment Processes on the Thermal Conductivity of an Al-Si-Cu-Fe-Zn Alloy. *Int. J. Heat Mass Transf.* **2017**, *105*, 189–195. [[CrossRef](#)]
124. Hu, C.; Zhao, H.; Wang, X.; Fu, J. Microstructure and Properties of AlSi12Fe Alloy High Pressure Die-Castings under Different Vacuum Levels. *Vacuum* **2020**, *180*, 109561. [[CrossRef](#)]
125. Liu, Y.; Zhang, Y.; Liu, W.; Jiao, X.; Nishat, H.; Ajavavarakula, D.; Chen, H.; Xiong, S. Enhanced Mechanical Properties and Thermal Conductivity of High-Pressure Die-Cast AlMg6Si2MnZr Alloy by Controlling the Externally Solidified Crystals. *J. Mater. Process. Technol.* **2022**, *306*, 117645. [[CrossRef](#)]
126. Hitchcock, M.; Wang, Y.; Fan, Z. Secondary Solidification Behaviour of the Al-Si-Mg Alloy Prepared by the Rheo-Diecasting Process. *Acta Mater.* **2007**, *55*, 1589–1598. [[CrossRef](#)]
127. Fan, Z. Semisolid Metal Processing. *Int. Mater. Rev.* **2002**, *47*, 49–85. [[CrossRef](#)]
128. Kirkwood, D.H. Semisolid Metal Processing. *Int. Mater. Rev.* **1994**, *39*, 173–189. [[CrossRef](#)]
129. Qi, M.; Kang, Y.; Zhu, G. Microstructure and Properties of Rheo-HPDC Al-8Si Alloy Prepared by Air-Cooled Stirring Rod Process. *Trans. Nonferrous Met. Soc. China* **2017**, *27*, 1939–1946. [[CrossRef](#)]
130. Lordan, E.; Zhang, Y.; Dou, K.; Jacot, A.; Tzileroglou, C.; Wang, S.; Wang, Y.; Patel, J.; Lazaro-Nebreda, J.; Zhou, X.; et al. High-Pressure Die Casting: A Review of Progress from the EPSRC Future LiME Hub. *Metals* **2022**, *12*, 1575. [[CrossRef](#)]
131. Arunkumar, K.; Bakshi, S.; Phanikumar, G.; Rao, T.V.L.N. Study of Flow and Heat Transfer in High Pressure Die Casting Cooling Channel. *Metall. Mater. Trans. B* **2023**, *54*, 1665–1674. [[CrossRef](#)]
132. Koru, M.; Serçe, O. Experimental and Theoretical Investigation of Heat Transfer in Vacuum Assisted High Pressure Die Casting (HPDC) Process. *Int. J. Met.* **2023**. [[CrossRef](#)]
133. Gautam, S.K.; Roy, H.; Lohar, A.K.; Samanta, S.K. Studies on Mold Filling Behavior of Al-10.5Si-1.7Cu Al Alloy During Rheo Pressure Die Casting System. *Int. J. Met.* **2023**, *17*, 2868–2877. [[CrossRef](#)]
134. Trometer, N.; Godlewski, L.A.; Prabhu, E.; Schopen, M.; Luo, A.A. Effect of Vacuum on Die Filling in High Pressure Die Casting: Water Analog, Process Simulation and Casting Validation. *Int. J. Met.* **2024**, *18*, 69–85. [[CrossRef](#)]
135. Dou, K.; Lordan, E.; Zhang, Y.; Jacot, A.; Fan, Z. A Novel Approach to Optimize Mechanical Properties for Aluminium Alloy in High Pressure Die Casting (HPDC) Process Combining Experiment and Modelling. *J. Mater. Process. Technol.* **2021**, *296*, 117193. [[CrossRef](#)]
136. Niu, Z.; Liu, G.; Li, T.; Ji, S. Effect of High Pressure Die Casting on the Castability, Defects and Mechanical Properties of Aluminium Alloys in Extra-Large Thin-Wall Castings. *J. Mater. Process. Technol.* **2022**, *303*, 117525. [[CrossRef](#)]
137. Cai, Q.; Mendis, C.L.; Wang, S.; Chang, I.T.H.; Fan, Z. Effect of Heat Treatment on Microstructure and Tensile Properties of Die-Cast Al-Cu-Si-Mg Alloys. *J. Alloys Compd.* **2021**, *881*, 160559. [[CrossRef](#)]
138. Tao, C.; Cheng, X.-N.; Li, Z.-Q.; Liu, G.-L.; Xu, F.-H.; Xie, S.-K.; Kuang, Z.-H.; Guo, Y.; Liu, H.-X. Mechanism of Cryogenic, Solid Solution and Aging Compound Heat Treatment of Die-Cast Al Alloys Considering Microstructure Variation. *Rare Met.* **2023**, *42*, 3130–3138. [[CrossRef](#)]
139. Zhang, J.; Cinkilic, E.; Huang, X.; Wang, G.G.; Liu, Y.; Weiler, J.P.; Luo, A.A. Optimization of T5 Heat Treatment in High Pressure Die Casting of Al-Si-Mg-Mn Alloys by Using an Improved Kampmann-Wagner Numerical (KWN) Model. *Mater. Sci. Eng. A* **2023**, *865*, 144604. [[CrossRef](#)]
140. Zhang, A.; Li, Y. Thermal Conductivity of Aluminum Alloys—A Review. *Materials* **2023**, *16*, 2972. [[CrossRef](#)]
141. Yuan, Z. Effect of Heat Treatment on Microstructure, Defects and Mechanical Properties of High Pressure Die Castings of Aluminum Alloys. Ph.D. Thesis, Tsinghua University, Beijing, China, 2019.
142. Han, Y.; Shao, D.; Chen, B.A.; Peng, Z.; Zhu, Z.X.; Zhang, Q.; Chen, X.; Liu, G.; Li, X.M. Effect of Mg/Si Ratio on the Microstructure and Hardness-Conductivity Relationship of Ultrafine-Grained Al-Mg-Si Alloys. *J. Mater. Sci.* **2017**, *52*, 4445–4459. [[CrossRef](#)]
143. Li, K.; Zhang, J.; Chen, X.; Yin, Y.; He, Y.; Zhou, Z.; Guan, R. Microstructure Evolution of Eutectic Si in Al-7Si Binary Alloy by Heat Treatment and Its Effect on Enhancing Thermal Conductivity. *J. Mater. Res. Technol.* **2020**, *9*, 8780–8786. [[CrossRef](#)]

144. Kim, Y.-M.; Choi, S.-W.; Kim, Y.-C.; Kang, C.-S. Influences of Heat Treatment on the Thermal Diffusivity and Corrosion Characterization of Al-Mg-Si alloy. *Korean J. Met. Mater.* **2021**, *59*, 582–588. [[CrossRef](#)]
145. Zhong, L.; Wang, Y.; Gong, M.; Zheng, X.; Peng, J. Effects of Precipitates and Its Interface on Thermal Conductivity of Mg–12Gd Alloy during Aging Treatment. *Mater. Charact.* **2018**, *138*, 284–288. [[CrossRef](#)]
146. Lumley, R.N.; Polmear, I.J.; Groot, H.; Ferrier, J. Thermal Characteristics of Heat-Treated Aluminum High-Pressure Die-Castings. *Scr. Mater.* **2008**, *58*, 1006–1009. [[CrossRef](#)]
147. Puzon, C.; Buttard, M.; Després, A.; Charlot, F.; Fivel, M.; Chehab, B.; Blandin, J.-J.; Martin, G. Direct Ageing of LPBF Al-1Fe-1Zr for High Conductivity and Mechanical Performance. *Acta Mater.* **2023**, *258*, 119199. [[CrossRef](#)]
148. Algendy, A.Y.; Javidani, M.; Khangholi, S.N.; Pan, L.; Chen, X.-G. Enhanced Mechanical Strength and Electrical Conductivity of Al–Ni-Based Conductor Cast Alloys Containing Mg and Si. *Adv. Eng. Mater.* **2024**, *26*, 2301241. [[CrossRef](#)]
149. Wang, J.; Carson, J.K.; North, M.F.; Cleland, D.J. A New Approach to Modelling the Effective Thermal Conductivity of Heterogeneous Materials. *Int. J. Heat Mass Transf.* **2006**, *49*, 3075–3083. [[CrossRef](#)]
150. Helsing, J.; Grimvall, G. Thermal Conductivity of Cast Iron: Models and Analysis of Experiments. *J. Appl. Phys.* **1991**, *70*, 1198–1206. [[CrossRef](#)]
151. Su, C. Thermal Mechanism of Magnesium Alloys Based on Solute Atom and Second Phase. Ph.D. Thesis, Shanghai Jiao Tong University, Shanghai, China, 2019.
152. Hamilton, R.L.; Crosser, O.K. Thermal Conductivity of Heterogeneous Two-Component Systems. *Ind. Eng. Chem. Fundam.* **1962**, *1*, 187–191. [[CrossRef](#)]
153. Vaney, J.-B.; Piarristeguy, A.; Ohorodniichuck, V.; Ferry, O.; Pradel, A.; Alleno, E.; Monnier, J.; Lopes, E.B.; Gonçalves, A.P.; Delaizir, G.; et al. Effective Medium Theory Based Modeling of the Thermoelectric Properties of Composites: Comparison between Predictions and Experiments in the Glass–Crystal Composite System $\text{Si}_{10}\text{As}_{15}\text{Te}_{75}\text{-Bi}_{0.4}\text{Sb}_{1.6}\text{Te}_3$. *J. Mater. Chem. C* **2015**, *3*, 11090–11098. [[CrossRef](#)]
154. Jiao, X.Y.; Wang, P.Y.; Liu, Y.X.; Jiang, J.J.; Liu, W.N.; Wan, A.X.; Shi, L.J.; Wang, C.G.; Xiong, S.M. Effect of Shot Speeds on the Microstructural Framework and Abnormal Eutectic Bands in a High Pressure Die Casting Hypoeutectic AlSi10MnMg Alloy. *J. Mater. Process. Technol.* **2024**, *326*, 118312. [[CrossRef](#)]

Disclaimer/Publisher’s Note: The statements, opinions and data contained in all publications are solely those of the individual author(s) and contributor(s) and not of MDPI and/or the editor(s). MDPI and/or the editor(s) disclaim responsibility for any injury to people or property resulting from any ideas, methods, instructions or products referred to in the content.